

Design of an IoT-enabled Scalable Closed Hydroponics System with
Smart Parameter Control

Exam Roll:

Registration No: 2018-526-853

Exam Roll:

Registration No: 2018-426-854

Session: 2018–2019



Department of Robotics and Mechatronics Engineering
University of Dhaka, Dhaka-1000, Bangladesh

January 6, 2024

Declaration of Authorship

We declare that this project titled, ‘Design of an IoT-enabled Scalable Closed Hydroponics System with Smart Parameter Control’ and the work presented in it are our own. We confirm that:

- This work was done wholly or mainly while in candidature for a B.Sc degree at this University.
- Where any part of this thesis has previously been submitted for a degree or any other qualification at this University or any other institution, this has been clearly stated.
- Where we have consulted the published work of others, this is always clearly attributed.
- Where we have quoted from the work of others, the source is always given. Except for such quotations, this project is entirely our own work.
- We have acknowledged all main sources of help.
- Where the project is based on work done jointly with others, we have clarified exactly what others did and what we contributed.

Countersigned:

(Professor Dr. Lafifa Jamal)
Supervisor

Signed:

(MD. Sameer Iqbal Chowdhury)
Candidate

Signed:

(Mikdam-Al-Maad Ronoue)
Candidate

Abstract

The need for controlled climate agriculture is becoming increasingly apparent due to climate change and global warming. Extreme and unpredictable weather poses a serious threat to the global food supply. As such, hydroponics is slowly emerging as an ideal alternative to traditional agriculture. Our proposed system seeks to build upon previous works in automated hydroponics and implement the monitoring and controlling of the key physical parameters responsible for the optimal growth of plants. Thus far, our system can control the pH, electrical conductivity and temperature of the nutrient solution as well as the temperature and humidity of the air present in the Growth Module. Additionally, the light cycle of the grow light installed in the system is also controlled. A web-based dashboard is also developed, which shows the sensor data from the system and can be accessed from any internet connection. In the future, we plan on extending the IoT capabilities of our system where we can instruct the system to monitor its physical parameters according to the type of plant being grown. An intelligent classification method will also be developed using Machine Learning to determine the control actions to be taken by the system depending on sensor data.

Acknowledgements

We would like to express our heartfelt gratitude to our esteemed professor, Dr. Lafifa Jamal, for her unwavering guidance and invaluable advice throughout the entirety of this project. Her expertise, patience, and unwavering support have been instrumental in shaping the direction and success of this endeavour. Dr. Jamal's dedication to our learning and development has been truly inspiring, and we are incredibly fortunate to have worked under her mentorship.

We would also like to express our immense gratitude to our respected faculty members Shifat-E-Arman and Jubair Ahmed, who have, at many points during this project, aided us with their practical knowledge and expertise in various research fields.

We also want to express our heartfelt appreciation to our friends and families who have stood by us throughout this journey. Their unwavering support, understanding, and encouragement have been the pillars of strength during challenging times. Their belief in our abilities and their constant words of encouragement have fueled our determination and kept us motivated.

Contents

| | |
|---|-----|
| Declaration of Authorship | i |
| Abstract | ii |
| Acknowledgements | iii |
| List of Figures | v |
| List of Tables | vi |
| 1 Introduction | 1 |
| 1.1 Classification of Hydroponic Systems | 2 |
| 1.2 Problem Definition | 3 |
| 1.3 Motivation | 4 |
| 1.4 Objectives | 5 |
| 2 Preliminaries | 6 |
| 2.1 Key Parameters for Plant Growth | 6 |
| 2.1.1 Nutrient Concentration | 6 |
| 2.1.2 Light Intensity and Cycle | 10 |
| 2.1.3 pH | 11 |
| 2.1.4 Temperature | 13 |
| 2.1.4.1 Air Temperature | 14 |
| 2.1.4.2 Water Temperature | 16 |
| 2.1.5 Humidity | 17 |
| 2.1.6 Carbon Dioxide(CO ₂) Concentration | 18 |
| 2.2 Smart Classification to Determine Control Actions | 19 |
| 2.3 Choice of Plant for The Proposed System | 24 |
| 3 Related Work | 25 |
| 3.1 Automated Hydroponic Greenhouse [70] | 25 |
| 3.1.1 Contributions | 26 |
| 3.1.2 Limitations | 27 |

| | | |
|---------|---|----|
| 3.2 | An Automated Hydroponics System Based on Mobile Application [72] | 27 |
| 3.2.1 | Contributions | 28 |
| 3.2.2 | Limitations | 28 |
| 3.3 | Hydroponic Nutrient Control System based on Internet of Things and K-Nearest Neighbors [73] | 28 |
| 3.3.1 | Contributions | 29 |
| 3.3.2 | Limitations | 30 |
| 3.4 | Fully Automated Hydroponic System for Indoor Plant Growth [12] | 30 |
| 3.4.1 | Summary | 30 |
| 3.4.2 | Contributions | 31 |
| 3.4.3 | Limitations | 32 |
| 3.5 | The Design and Implementation of a Hydroponics Control System [74] | 32 |
| 3.5.1 | Contributions | 33 |
| 3.5.2 | Limitations | 33 |
| 3.6 | IoT based hydroponics system using Deep Neural Networks [59] | 33 |
| 3.6.1 | Contributions | 35 |
| 3.6.2 | Limitations | 35 |
| 3.7 | Automated system developed to control pH and concentration of nutrient solution evaluated in hydroponic lettuce production [75] | 36 |
| 3.7.1 | Summary | 36 |
| 3.7.2 | Contributions | 38 |
| 3.7.3 | Limitations | 38 |
| 3.8 | Observations from Related Works and Conclusion | 39 |
| 4 | Methodology | 41 |
| 4.1 | Proposed System | 41 |
| 4.1.1 | System Modules | 41 |
| 4.1.2 | IoT Environment | 45 |
| 4.2 | Work Done Already | 48 |
| 4.2.1 | 3D CAD Model | 48 |
| 4.2.2 | Physical Structure | 53 |
| 4.2.3 | Sensors | 56 |
| 4.2.3.1 | Initial Approach of Calibration and Placement of a Low-end pH Sensor | 56 |
| 4.2.3.2 | Current Approach of Using the Atlas Scientific pH Kit | 58 |
| 4.2.3.3 | Placement of Air Temperature and Humidity Sensor | 60 |
| 4.2.3.4 | Placement of Water Temperature Sensor | 60 |
| 4.2.3.5 | Initial Approach of the Calibration and Placement of TDS/EC Sensor | 61 |
| 4.2.3.6 | Current Approach of Using the Atlas Scientific Mini Conductivity K 1.0 Kit | 64 |
| 4.2.3.7 | Placement of Water Level Sensor | 66 |

| | |
|--|----|
| 4.2.3.8 Placement of CO ₂ Sensor | 66 |
| 4.2.4 Actuators | 66 |
| 4.2.4.1 Initial Solution Cooling Approach with the Thermoelectric Peltier Water Cooler | 66 |
| 4.2.4.2 Current Approach of Using a Refrigerative Cooler | 68 |
| 4.2.4.3 Thermoelectric Peltier Air Cooler | 70 |
| 4.2.4.4 Initial Approach for the Nutrient and Acid/Base Dosing System | 72 |
| 4.2.4.5 Current Approach for the Nutrient and Acid/Base Dosing System | 74 |
| 4.2.4.6 Automated Multi-plug for High Power Components | 75 |
| 4.2.4.7 Grow Lights | 76 |
| 4.2.4.8 CO ₂ Gas Delivery System | 77 |
| 4.2.5 Electrical System Schematic | 78 |
| 4.2.5.1 Sensor Board Design | 78 |
| 4.2.5.2 Actuator Board Design | 80 |
| 4.2.6 Microcontrollers | 80 |
| 4.2.6.1 Using a Raspberry Pi 4 as the Central Control Unit | 80 |
| 4.2.6.2 Using a Raspberry Pi as an Internet of Things (IoT) Gateway | 81 |
| 4.2.7 Current Setup of the System | 84 |
| 4.2.7.1 Trial Run of the System | 85 |
| 4.3 Expected work to be done | 85 |
| 4.3.1 Adding CO ₂ and its controls to the Growth Module | 85 |
| 4.3.2 Building multiple GMs and integrating them into the existing system | 86 |
| 5 Results | 87 |
| 5.1 Real-time Monitoring of the Physical Parameters | 87 |
| 5.2 Collection of Sensor Data in Google Sheets for Current Database and Future Dataset | 90 |
| 6 Conclusion | 91 |
| Bibliography | 93 |
| Appendix A: List of Acronyms | 93 |

List of Figures

| | | |
|------|---|----|
| 1.1 | Simplified diagram of an NFT System [6] | 3 |
| 2.1 | Atlas Scientific Mini Conductivity K 1.0 Kit [26] | 9 |
| 2.2 | Auoyo 40W LED Growlight Lamps [34] | 11 |
| 2.3 | BH1750 Ambient Light Sensor [35] | 11 |
| 2.4 | Atlas Scientific Analog pH Kit [39] | 12 |
| 2.5 | DHT22 Temperature and Humidity Sensor [45] | 15 |
| 2.6 | Working principle of the DHT22 Temperature and Humidity Sensor [46] | 15 |
| 2.7 | Waterproof 1-Wire DS18B20 Digital temperature sensor [50] | 16 |
| 2.8 | MH-Z19C NDIR CO ₂ Module [57] | 18 |
| 2.9 | Illustrated example of a Decision Tree from the root node to leaf nodes [63] | 21 |
| 2.10 | Illustration of bagging ensemble learning algorithm [64] | 21 |
| 2.11 | Illustration of the Random Forest algorithm [64] | 22 |
| 2.12 | Illustration of the Boosting ensemble algorithm [64] | 22 |
| 2.13 | Illustration of the XGBoost algorithm [66] | 23 |
| 3.1 | System Block Diagram [71] | 26 |
| 3.2 | System Overview [72] | 28 |
| 3.3 | System Architecture [58] | 29 |
| 3.4 | Hardware components of the system [12] | 31 |
| 3.5 | Different sensors and parameter inducers [12] | 31 |
| 3.6 | Overall view of the system [74] | 32 |
| 3.7 | System architecture of IoT based hydroponics [59] | 34 |
| 3.8 | Data flow diagram [59] | 34 |
| 3.9 | Flowchart of instrumental system developed by DIA/UEL Group, utilized in monitoring and control of hydroponic lettuce. V1, V2 and V3 are solenoid valves [75] | 37 |
| 3.10 | Digitized screen of software ControlHidro and image of automated hydroponic cultivation obtained through a webcam by remote connection [75] | 38 |
| 4.1 | Simplified outline of the system | 42 |
| 4.2 | Block diagram for the Nutrient Solution Container Module | 43 |
| 4.3 | Block diagram for the Growth Module | 44 |
| 4.4 | Block diagram for the IoT framework of the system | 46 |

| | | |
|------|---|----|
| 4.5 | Block diagram for communication between the Arduino microcontrollers and the Raspberry Pi | 47 |
| 4.6 | Flow diagram for the entire system | 48 |
| 4.7 | Overhead view of the 3D CAD model of the system | 49 |
| 4.8 | Left view of the 3D CAD model of the system | 49 |
| 4.9 | Top view of the 3D CAD model of the system | 50 |
| 4.10 | Front view of the 3D CAD model of the system | 50 |
| 4.11 | Right view of the 3D CAD model of the system | 51 |
| 4.12 | 3D model of pH probe holder clamp | 52 |
| 4.13 | 3D model of pH probe holder clamp head | 52 |
| 4.14 | 3D model of pH probe holder clamp head | 53 |
| 4.15 | 3D model of EC probe holder clamp | 53 |
| 4.16 | Top view of the physical structure | 54 |
| 4.17 | Front view of the physical structure | 54 |
| 4.18 | Right view of the physical structure | 55 |
| 4.19 | Water flowing from the 3-inch uPVC pipe back to the NSCM via the 1.5-inch suction hose | 55 |
| 4.20 | Ultrasonic sensor, pH probe, TDS probe and temperature probe held above the nutrient solution by the sensor holders | 56 |
| 4.21 | Scatter-plot of pH against electrode voltage graph, plotted in Seaborn | 57 |
| 4.22 | Atlas Scientific pH sensor probe fixed on the sensor holder and immersed in nutrient solution | 60 |
| 4.23 | DHT22 sensor mounted on the side wall of the Growth Module | 60 |
| 4.24 | Scatterplot of EC against electrode voltage graph, plotted in Seaborn | 63 |
| 4.25 | Atlas Scientific EC sensor probe fixed on the sensor holder and immersed in nutrient solution | 65 |
| 4.26 | HC-SR04 Ultrasonic sensor [80] | 66 |
| 4.27 | MH-Z19C NDIR CO₂ sensor mounted on the side wall of the Growth Module | 67 |
| 4.28 | Lenovo Select FHD Webcam mounted near the top corner of the Growth Module | 67 |
| 4.29 | Block diagram for the thermoelectric Peltier cooler | 68 |
| 4.30 | Top view of Thermoelectric Peltier Module-based Water Cooler . . | 69 |
| 4.31 | Side view of Thermoelectric Peltier Module-based Water Cooler . . | 69 |
| 4.32 | Hailea HS-28A Aquarium Chiller placed beside the NSCM | 71 |
| 4.33 | Block Diagram for the thermoelectric Peltier Air Cooler | 72 |
| 4.34 | Air Cooler attached to the side of the GM | 73 |
| 4.35 | Air Cooler attached to the side of the GM | 73 |
| 4.36 | SMPS 30A Power Supply | 74 |
| 4.37 | Block diagram of the dosing system | 75 |
| 4.38 | Nutrient and Acid/Base Dosing System | 76 |
| 4.39 | Top view of the new Dosing System | 77 |
| 4.40 | Side view of the new Dosing System | 77 |
| 4.41 | Automated Multiplug | 78 |

| | | |
|------|---|----|
| 4.42 | Grow Lights mounted under the lid of the Growth Module | 79 |
| 4.43 | CO ₂ delivery system. The CO ₂ cylinder (left) is connected via tubing to the GM (right) | 80 |
| 4.44 | Schematic for the sensor board, designed in Proteus 8 Professional . | 80 |
| 4.45 | Top view of the sensor board | 81 |
| 4.46 | Bottom view of the sensor board | 82 |
| 4.47 | The top view of the actuator board (left) and the bottom view of the actuator board (right), which shows the soldered connections between the pins of the Arduino Mega and the JST connector pins . | 82 |
| 4.48 | Raspberry Pi connected with the Arduino Nano and Arduino Mega | 83 |
| 4.49 | Block diagram illustrating the flow of data between the Raspberry Pi, Arduino microcontrollers and ThingSpeak | 84 |
| 4.50 | Web-based dashboard showing the visualizations from ThingSpeak from sensor data | 85 |
| 4.51 | Web-based dashboard showing the widgets from ThingSpeak from sensor data | 85 |
| 4.52 | Front view of the metal frame housing the NSCM and supporting the GM | 86 |
| 4.53 | Front view of the current setup of the system | 86 |
| 4.54 | Leaf area of a plant being measured using FIJI | 88 |
| 5.1 | Graphs on the web-based dashboard show the initial values taken by the sensors | 91 |
| 5.2 | Widgets on the web-based dashboard show the initial values taken by the sensors | 91 |
| 5.3 | Graphs on the web-based dashboard show the values settling down taken by the sensors | 92 |
| 5.4 | Graphs on the web-based dashboard show the values settling down taken by the sensors | 92 |
| 5.5 | Google Sheet showing the sensor data being stored along with timestamps | 93 |

List of Tables

| | | |
|-----|--|----|
| 2.1 | Contents of Concentrated Nutrient Solution A [21] | 7 |
| 2.2 | Contents of Concentrated Nutrient Solution B [21] | 8 |
| 2.3 | Optimal Growth Parameter Values For Lettuce [69] | 24 |
| 3.1 | Tabular comparison of the related works | 39 |
| 4.1 | Voltage readings from pH probe calibration with buffer solutions of pH 4.00, 6.86, and 9.19 | 57 |
| 4.2 | List of calibration commands sent to the Atlas Scientific pH Kit . . | 59 |
| 4.3 | Voltage readings from TDS probe calibration with 32 sample solutions with different TDS values | 62 |
| 4.4 | List of calibration commands sent to the Atlas Scientific Mini Conductivity K 1.0 Kit | 65 |

Chapter 1

Introduction

With the onset of global warming, one of the biggest challenges the world will face is an impending global food shortage. By 2050, we will need to increase food production by about 70% to meet the caloric needs of a population of 9.8 billion—68% of whom are estimated to live in urban areas. If we were to project linear growth in yield from our agricultural output from the past five decades, we would be nowhere near achieving this kind of growth by 2050. Not to mention, the enormous demand for water in agriculture is ever-increasing. Globally, 70% of water usage goes towards agricultural production, largely due to unsustainable irrigation practices [1]. This has brought to question conventional agricultural practices, which are quite resource intensive while proving to be an unreliable food source for the world population. Experts have since explored alternative farming practices to develop viable and sustainable agricultural techniques to match the increasing demand for food. One such practice is hydroponic agriculture.

Hydroponics is the growing of plants in an aqueous nutrient solution with or without the use of non-soil media. Commonly used mediums include expanded clay, coir, perlite, vermiculite, brick shards, polystyrene packing peanuts, and wood fiber [2].

This form of agriculture removes the traditional dependence on arable land, often a significant limiting factor for a region's agricultural output. Hydroponic systems are also ideal for smaller spaces such as balconies and rooftops where it would otherwise be difficult to grow anything via conventional methods [3].

1.1 Classification of Hydroponic Systems

Hydroponic systems can be classified into two categories:

1. Static solution culture system, where the plants are cultivated in containers where the nutrient solution is kept below the plants' root level or just about in contact with them. The solution is gently aerated to allow the inflow of oxygen into the solution, although it can also be left unaerated. If the solution is not aerated, the solution level is kept low enough so enough roots are above the solution to receive an adequate oxygen concentration. A single container might be used for a single or a multitude of plants. The reservoir size may be changed per the growth of the plants. The nutritional solution is replaced regularly, such as once a week or when the concentration falls below a specified level, as indicated by an electrical conductivity(EC) meter. When the concentration falls below the specified level, the nutrient solution must be replaced, or new nutrients must be added to maintain a proper supply of nutrients to the plants.
2. Continuous-flow solution culture system where the nutrient solution constantly flows between the plants and a reservoir in this system. One single reservoir can be used to deliver nutrient solution to a large number of plants or containers. It is also easier to maintain the temperature, pH, and nutrient concentration of the solution in this system compared to the static solution culture system.

Hydroponic systems that are closed (i.e., the plants are placed inside a system with a controlled environment) also benefit from being significantly less likely to attract pest infestations [4]. This effectively eliminates the need for pesticides. This makes produce from such systems much safer and healthier to consume.

Among the continuous-flow solution systems, Nutrient Film Technique (NFT) systems are widely used for small-scale home setups and agricultural systems. The idea behind the NFT system consists of recirculating the nutrient solution stored in a reservoir using an electric water pump through PVC pipes, which act as growing channels to hold and allow the plants to grow [5]. The growing channels are

supported at an elevated slope to facilitate nutrient solution circulation along the channels. A thin layer of the nutrient solution runs through the growing channels, giving it the term “film” because of its thin nature. Due to its closed nature, it is regarded as a continuous re-circulation system. This continuous flow of nutrient solution onto the roots of the plants ensures that the required nutrients are available to the plants at all times, including oxygen which is dissolved in aerated systems. The nutrient solution is drained from the growth channels and sent back to the tank where the nutrient solution is primarily stored. This allows the nutrient solution to remain in constant circulation throughout the entire system as the electric pump runs around the clock [5].

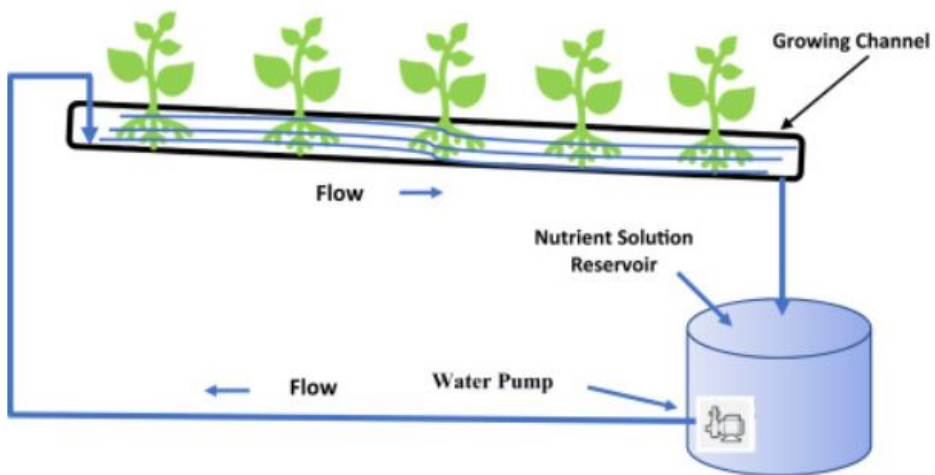


Figure 1.1: Simplified diagram of an NFT System [6]

1.2 Problem Definition

Hydroponic methods have been studied and improved significantly over the years. Areas of improvement include incorporating vertical farming, the practice of growing crops in layers stacked vertically [7]. Various research has been carried out to design and build automatic hydroponic systems, where a control system is set in place to measure and control the plants’ growth parameters (i.e., air temperature, water temperature, humidity, pH, nutrient level, light cycle/intensity, CO₂ concentration) to ensure optimal growth of the plants [8]. However, there is an

existing limitation among these systems as none consider all the parameters for a plant's growth. This greatly limits the growth rate of the plants. Similarly, none of the existing studies incorporates the aspect of growing various species of plants simultaneously in the same hydroponic system.

1.3 Motivation

Hydroponics has the potential to revolutionize global agriculture. Large-scale adaptations of this subset of agriculture would significantly reduce the burden on existing arable land and cease searches for newer arable lands, which lead to deforestation and ecological destruction [9], all the while tackling an emerging global food crisis [10].

However, the existing systems cannot provide the optimal conditions for the plants' growth within the shortest possible time. CO₂ concentration, in particular, is a parameter that none of the previous works has successfully attempted to control. This parameter is of particular interest in our proposed system since increased ambient CO₂ concentration over the years has been linked to greater growth among plants [11].

Secondly, the systems are also designed to allow one specific plant species to grow within the system at a given time.

Furthermore, with the additional implementation of Internet of Things (IoT) in some studies, such as [12], only some parameters are monitored. However, the control systems are not designed to respond to user inputs.

Our proposed idea is to create an automated hydroponics system, which will be a closed, climate-controlled system where we can vary all the parameters known to contribute to plant growth [8]. Having complete control of the interior weather of the system, we can adjust the parameters to allow almost every plant that grows and bears fruit above the soil level. Furthermore, the system will be built inside containers, allowing us to create multiple units; each with an environment optimized per the unique requirements of different types of plants in which they thrive [13], or all of them catered to the production of a single plant type in large

volume. The containers will be operated independently via their microcontrollers, with a central server monitoring all containers simultaneously. The later parts of this report will cover the extensive review of the existing works in hydroponics, our proposed system's methodology, and our implementation of the aforementioned design up to this point.

1.4 Objectives

The objectives of this project are as follows:

- To design a closed-system automated hydroponic system that monitors and controls all the growth parameters of a plant (i.e., air temperature, water temperature, humidity, pH, nutrient level, light cycle/intensity, CO₂ concentration) [8].
- To design the system to have an external source of CO₂ gas while measuring and controlling its concentration safely.
- To make the system easily scalable with multiple growth containers, each allowing different species of plants to grow while being controlled by a central server.
- To create an IoT framework that allows users to monitor the growth parameters of the plant as well as its current state via real-time video feedback and control the system remotely per requirement.

Chapter 2

Preliminaries

Our proposed system aims to work with the physical conditions that determine plants' overall growth. Thus, we will start this chapter by defining the physical conditions monitored and controlled within our system.

2.1 Key Parameters for Plant Growth

The growth of plants is affected by seven primary parameters. Below, we define them in-depth while expanding on how they affect plant growth:

2.1.1 Nutrient Concentration

Plants typically require 14 mineral elements for proper nutrition and growth. These include the 6 macronutrients (nutrients that are required in relatively greater concentrations): Nitrogen (N), Phosphorus (P), Potassium (K), Calcium (Ca), Magnesium (Mg), and Sulphur (S), and micronutrients (nutrients that are required in relatively greater concentrations): Chlorine (Cl), Boron (B), Iron (Fe), Manganese (Mn), Copper (Cu), Zinc (Zn), Nickel (Ni) and Molybdenum (Mo) [14].

Among the macronutrients listed, Nitrogen (N), Phosphorus (P), and Potassium (K) are the primary nutrients needed by plants to develop properly [15]. In studies

where NPK-based fertilizers were added to soil, a marked increase in growth rate was observed in the plants where the fertilizer was applied, compared to plants that were not treated with it [16], as well as when compared with the application of organic green manure [17].

Conventionally in soil-based agriculture, nitrogen is made available to the plants through nitrates mixed in the soil, further broken down by symbiotic bacteria to provide nitrogen to the plant roots [18]. The plant roots take up phosphate ions in the soil for phosphorus, mostly using diffusion [19]. For potassium, potassium ions in the soil are absorbed into the plant roots [20]. In hydroponics, the principles of nutritional uptake by the plant remain the same. Nutrients are dissolved in water, in which the plant roots are submerged.

The nutrients are introduced into a hydroponics system with the application of standard nutrient solutions which are commercially known as nutrient solution A and B. The chemical composition of these solutions is given in Table 2.1 and 2.2.

| Concentrated Nutrient Solution A | |
|----------------------------------|-------------------------------------|
| Component | Concentration (g L^{-1}) |
| KNO_3 | 45.30 |
| $\text{Ca}(\text{NO}_3)_2$ | 26.70 |
| NH_4NO_3 | 1.33 |
| Fe-chelate (6%) | 3.00 |

Table 2.1: Contents of Concentrated Nutrient Solution A [21]

| Concentrated Nutrient Solution B | |
|----------------------------------|-------------------------------------|
| Component | Concentration (g L^{-1}) |
| KH_3PO_4 | 20.00 |
| MgSO_4 | 20.00 |
| K_2SO_4 | 15.30 |
| KNO_3 | 14.70 |
| MnSO_4 | 0.16 |
| ZnSO_4 | 0.23 |
| B | 0.23 |
| CuSO_4 | 0.03 |
| Na_2MoO_4 | 0.01 |

Table 2.2: Contents of Concentrated Nutrient Solution B [21]

In a hydroponics system, distilled water dissolves the required nutrients to prepare the nutrition solution. The ionic nutrients dissociate to form cations and anions, allowing for a certain conductivity level of electric current in the solution. This phenomenon is electrical conductivity (EC) [22]. There is a direct relationship between the EC of a solution and the concentration of ions present in the solution [23].

Instead of measuring EC directly, we measure the Total Dissolved Solids (TDS) in the nutrient solution in our proposed system. For varying levels of TDS, the EC of the nutrient solution be measured using linear relationships [24]. The presence of ions in the nutrient solution leads to a rise in potential difference across the electrodes of the TDS sensor. The potential difference reading is transmitted to an Arduino microcontroller for our proposed system. The readings are then calibrated to TDS readings and converted to EC readings using linear relationships, where the TDS value is the independent variable.

Equation 2.1 shows this linear relationship:

$$\text{Electrical Conductivity} = \alpha \times \text{Total Dissolved Solids (TDS)} \quad (2.1)$$

α is the conversion factor which typically has a value of 0.5 [25].

Our proposed system uses an Atlas Scientific Mini Conductivity K 1.0 Kit, as seen in Figure 2.1.



Figure 2.1: Atlas Scientific Mini Conductivity K 1.0 Kit [26]

A Total Dissolved Solids (TDS) or Electrical Conductivity (EC) meter uses a conductivity probe to generate an electrical charge when immersed into a solution. A change in the number of dissolved ions will lead to a corresponding change in the electrical charge magnitude. The measurement of charge can be taken by a conductivity meter, consequently determining the conductance of the solution.

Upon immersion of the probe into the solution, an electric current is established between the two electrodes within the probe, which are positioned at a fixed distance. The concentration of ions present determines the conductance of a solution. A higher ion concentration increases conductance, resulting in a greater current flow. A decrease in current leads to a reduction in the conductance value, as this is attributed to a decrease in the concentration of ions within the solution [27].

The TDS sensor was used to measure the EC of the nutrient solution since both measure the concentration of ions in a solution and are related by Equation 2.1.

2.1.2 Light Intensity and Cycle

Plants rely heavily on sunlight for their growth and development due to its essential role in photosynthesis. It is a complex biochemical mechanism through which plants convert light energy into chemical energy, enabling them to synthesize organic compounds necessary for survival.

Within specialized cellular structures called chloroplasts, plant pigments, such as chlorophyll, absorb and capture light energy. This absorbed energy converts carbon dioxide and water into glucose and oxygen. The availability of an adequate amount of sunlight directly impacts the efficiency of photosynthesis. Insufficient sunlight can hinder this energy-conversion process, reducing plant growth, diminishing vitality, and compromising overall health [28].

Studies have established a positive relationship between light intensity and the growth rate and biomass of plants [29], [30]. Each plant species has a set range of light intensity at which it grows the best, along with varying light intensities and wavelengths at which the plants have optimal plant height, dry biomass, leaf area, and the number of branches [31].

The effects of different light cycles have also been studied, indicating that longer cycles of light and darkness, such as 12 hours of light followed by 12 hours of darkness, ensure optimal growth rate for plants[32]. Modern greenhouses have grow lights designed to emit Red and Blue lights. These two wavelengths on the visible light spectrum contribute the most toward plant growth [33].

Our proposed system is equipped with two Auoyo 40W LED Growlight lamps, which can be seen in Figure 2.2. The lamps are embedded with Light-Emitting-Diodes(LEDs), emitting red and blue light. The ratio of red to blue LEDs is fixed by the company to ensure the balanced and optimal growth of plants across all stages of growth, starting from the seedling stage to the vegetative and flower/fruit stages.

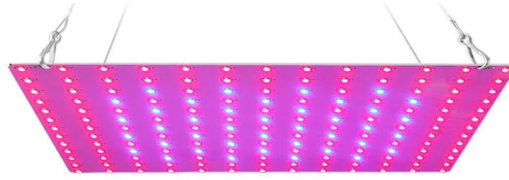


Figure 2.2: Auoyo 40W LED Growlight Lamps [34]

The on/off action of the lamps is timed by the Arduino. Using the `Millis()` function from its in-built libraries, the Arduino times the duration for which the lamps will be kept on and off. The current state of the lamp is monitored using a BH1750 Ambient Light Sensor, as seen in Figure 2.3.



Figure 2.3: BH1750 Ambient Light Sensor [35]

2.1.3 pH

Potential Hydrogen(pH) measures how acidic or basic a substance is. The following Equation 2.2 gives the value of pH:

$$\text{pH} = -\log_{10}[\text{H}^+] \quad (2.2)$$

$[\text{H}^+]$ is the concentration of H^+ ions in mol L^{-1} present in the solution. pH has a typical range of 0 to 14. A pH value of 0 indicates most acidic, 14 indicates most basic, and 7 indicates that the substance is neutral, meaning it is neither basic nor acidic [36]. The optimal pH for plants differs at each stage of their lifespan as well as across species, and its effect on their growth is profound [37].

At high pH levels, the concentration of zinc present in the soil, or nutrient solution in our case, decreases. Similarly, the concentration of phosphorus and molybdenum

decreases at low pH levels. Thus, it is imperative to maintain a fixed range of pH of the nutrient solution to provide the plants with their required nutrients up to adequate levels [38].

Our proposed system uses an Altas Scientific pH Kit, as seen in Figure 2.4.



Figure 2.4: Atlas Scientific Analog pH Kit [39]

This kit is popularly used with Arduino and Raspberry Pi modules. The kit comes with the following [39]:

1. A high-quality pH probe attached to a BNC connector. The probe consists of a glass electrode that generates a voltage proportional to the measured pH level of the submerged solution.
2. A signal conversion circuit board amplifies and conditions the pH probe's signal to make it compatible with the analog input of the Arduino board. It also provides temperature compensation to ensure accurate pH readings across various temperatures.
3. A Electrically Isolated EZOTM Carrier Board. The board allows seamless connection of EZOTM sensors to microcontrollers or single-board computers through serial communication interfaces while ensuring complete electrical separation between the sensor circuit and the host system. This isolation prevents the flow of electrical currents between the two circuits, eliminating potential issues such as noise interference and ground loops.

4. Connector cables that connect the pH probe and the signal conditioning board to the Arduino board easily. The cables comprise 3 wires: Ground, V_{cc} and Analog Signal Output.

pH probes are equipped with two electrodes housed within the probe body: a measuring electrode, commonly called the glass electrode, and a reference electrode. The glass electrode has a reference electrolyte, typically potassium chloride, with a pH value of 7, signifying its neutrality. Consequently, the reference electrolyte contains a precise quantity of hydrogen ions.

The glass electrode functions by quantifying the disparity in pH levels between the pH electrode and the solution under examination. The electrode accomplishes this by quantifying the disparities in voltage between the hydrogen ions generated within the electrode and the surrounding solution. Determining the pH value of the glass electrode composition facilitates the ease of calculation.

When immersing a pH probe into a solution, migration of hydrogen ions towards the glass electrode occurs, leading to the displacement of certain metal ions within the electrode. Simultaneously, a portion of the hydrogen ions will disperse into the solution. The phenomenon of ion swapping is commonly referred to as ion exchange and serves as the fundamental principle underlying the functionality of the glass electrode housed within a pH probe.

Ion exchange is also observed within the internal surface of the glass electrode. The dissimilarity in acidity between the potassium chloride within the electrode and the solution under examination leads to a disparity in hydrogen-ion activity, thereby generating a discrepancy in electrical charges. When this phenomenon occurs, an electrical potential difference arises between the surfaces of the glass electrode and the reference electrode, resulting in a pH measurement on the meter [39].

2.1.4 Temperature

Temperature plays a crucial role in plant functions such as photosynthesis, transpiration, respiration, germination, and flowering. As the temperature rises (within

a certain range), photosynthesis, transpiration, and respiration rates also increase. Additionally, when the temperature is considered in conjunction with the length of daylight, it influences the shift from vegetative growth, which focuses on leaves, to reproductive growth centered around flowering. The impact of temperature on this transition can either accelerate or decelerate depending on the specific plant and the environmental conditions [40].

In hydroponics, temperature is broken down into two sections: temperature of the air in contact with the plant above root or ground level and temperature of the water in which the plant's roots remain submerged [41].

2.1.4.1 Air Temperature

Air temperature, conventionally referred to as just temperature in traditional agriculture, plays a crucial role in the growth and development of plants. It influences various physiological and biochemical processes in plants, from germination of seeds to photosynthesis in the leaves to flowering, ultimately affecting their growth [42]. Warmer temperatures generally promote faster photosynthesis rates and increase plants' overall metabolic activity. This can lead to accelerated growth, especially during the growing season [43].

However, excessively high temperatures can harm plant growth, causing heat stress and impairing key physiological functions. Conversely, extremely low temperatures can also hinder plant growth by reducing metabolic activity and damaging plant tissues. Therefore, maintaining optimal air temperature is essential for maximizing plant growth and productivity. The optimal air temperature varies from plant to plant and even during the different stages of a plant's life cycle [44].

Our proposed system uses a DHT22 Temperature and Humidity Sensor, as seen in Figure 2.5.

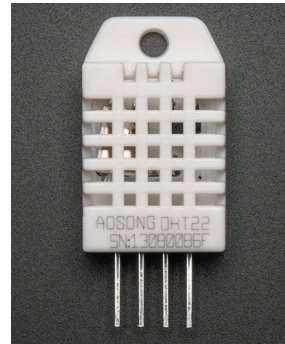


Figure 2.5: DHT22 Temperature and Humidity Sensor [45]

This highly popular and low-cost sensor is used with popular microcontrollers such as Arduino and Raspberry Pi modules. The sensor has two sections:

1. A Negative-Temperature-Coefficient(NTC) thermistor. For a positive temperature change, the resistance across the thermistor drops, thus creating a decreasing graph of resistance against temperature, as illustrated in Figure 2.6. The Integrated Circuit (IC) present in the sensor uses the analog resistance from the thermistor. It converts it into digital temperature readings, which it transmits to the microcontroller.
2. A capacitive humidity sensor designed to have two electrode plates with moisture-holding substrate between them, as illustrated in Figure 2.6. Ambient humidity alters the amount of moisture absorbed into the substrate, affecting the capacitor-like sensor's conductance and leading to a change in voltage across the two electrodes. The IC converts this analog voltage into digital humidity readings and transmits them to the microcontroller [46].

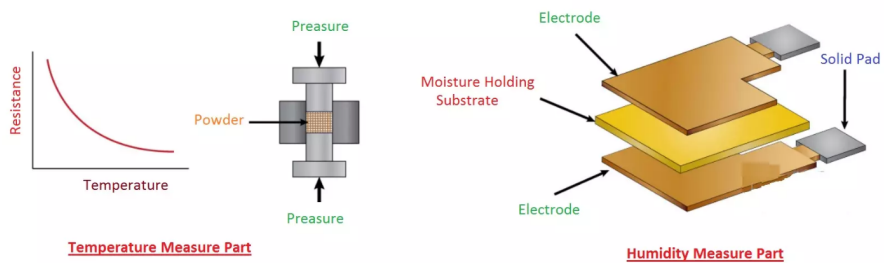


Figure 2.6: Working principle of the DHT22 Temperature and Humidity Sensor

[46]

The DHT22 sensor has 3 pins: Ground, V_{cc} and Digital Signal Output. It has an operating voltage of 3.0 to 5.5V, a temperature reading range of -40°C to 80°C with $\pm 0.5^\circ\text{C}$ accuracy, a humidity reading range of 20% to 80% with $\pm 1\%$ accuracy and a settling time of 2 seconds [45].

2.1.4.2 Water Temperature

The temperature of water has significant implications for the growth of plants. Water temperature affects plant nutrient uptake, metabolic activity, and biochemical reactions. Warmer water temperatures generally enhance nutrient absorption and enzymatic processes, enabling faster growth rates [47].

Conversely, colder water temperatures can slow down plant metabolism [48], leading to reduced growth and nutrient uptake. Extreme temperatures, whether too hot or too cold, can cause stress and damage to plant cells [49]. Therefore, maintaining the optimal water temperature is crucial for optimizing plant growth and ensuring their overall health and productivity and subsequent nutritional value.

Our proposed system uses a Waterproof 1-Wire DS18B20 Digital temperature sensor, as seen in Figure 2.7.



Figure 2.7: Waterproof 1-Wire DS18B20 Digital temperature sensor [50]

The DS18B20 Digital temperature sensor uses a Temperature-to-digital converter, wherein the voltage change across the diode's junctions is used to determine the temperature change, establishing a proportional relationship between them [51].

The DS18B20 Digital temperature sensor has 3 pins: Ground, V_{cc} and Digital Signal Output. It has an operational voltage of 3.0 to 5.5V, a temperature measurement range of -55°C to +125°C with an accuracy of $\pm 0.5^\circ\text{C}$ [52].

2.1.5 Humidity

Humidity is a measure of the concentration of water vapor present in the air. Humidity is measured as absolute and relative humidity(RH). For our proposed system, we consider relative humidity, which is given by Equation 2.3:

$$\text{Relative Humidity (RH)} = \frac{\rho_w}{\rho_s} \times 100\% \quad (2.3)$$

ρ_w is the density of water vapour in the air, ρ_s is the density of water vapour at saturation. The level of atmospheric humidity plays a significant role in the growth and development of plants. Humidity affects plant transpiration, stomatal conductance, which is a measure of how open the stomata of a leaf are, and water uptake, all of which directly impact plant growth. Higher humidity levels can reduce water loss through transpiration, allowing plants to conserve moisture and maintain optimal hydration. This can promote efficient nutrient uptake and photosynthesis, leading to healthier growth [53].

On the other hand, extremely low humidity can increase transpiration rates and cause water stress in plants, hindering their growth and potentially leading to leaf wilting. Therefore, maintaining optimal humidity levels based on plant species, plant life cycle and environmental conditions is crucial for supporting optimal growth and ensuring plant vitality.

The humidity of the system is measured using the DHT22 Temperature and Humidity sensor.

2.1.6 Carbon Dioxide(CO_2) Concentration

Carbon dioxide(CO_2) concentration has a significant impact on the growth of plants. Increased levels of CO_2 in the atmosphere can stimulate photosynthesis, the process by which plants convert CO_2 and sunlight into energy [54]. Higher concentrations of CO_2 enhance the availability of this essential building block, resulting in improved plant growth, biomass production, and yield [55].

Additionally, elevated CO_2 levels often reduce plant water loss through stomatal closure, promoting water-use efficiency [56]. However, the effects of increased CO_2 can vary among plant species, nutrient availability, and other environmental factors. Therefore, the other growth parameters must also be considered while settling on an optimal CO_2 concentration for specific types of plants, as well as during different phases of their life cycle.

Our proposed system uses an MH-Z19C NDIR CO_2 Module, as seen in Figure 2.8.

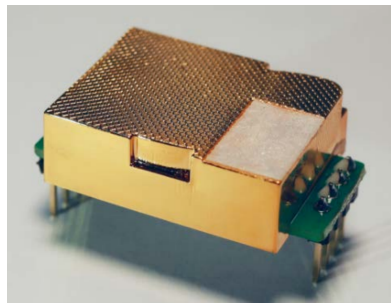


Figure 2.8: MH-Z19C NDIR CO_2 Module [57]

The MH-Z19C infrared CO_2 sensor operates on the fundamental principles of non-dispersive infrared (NDIR) gas detection. At its core, the sensor employs an infrared light source, a gas sample chamber, and an infrared detector to quantify the concentration of carbon dioxide in the surrounding environment.

The process begins with the emission of infrared light by the light source of the sensor. This light passes through the gas sample chamber, which contains the air to be analyzed. Carbon dioxide molecules in the chamber absorb specific wavelengths of infrared light in proportion to their concentration. The remaining light, unaffected by CO_2 absorption, reaches the infrared detector.

The detector then measures the intensity of the transmitted light and generates a corresponding electrical signal. By analyzing the reduction in light intensity caused by CO₂ absorption, the sensor can accurately determine the concentration of carbon dioxide present in the sampled air.

One of the key advantages of the MH-Z19C lies in its ability to provide precise and reliable CO₂ measurements with minimal interference from other gases. This is achieved by carefully selecting the infrared wavelengths used for detection, allowing the sensor to target CO₂ molecules specifically. Furthermore, the sensor incorporates calibration algorithms to enhance accuracy over various environmental conditions. Regular calibration ensures that the sensor maintains its reliability and remains sensitive to changes in CO₂ levels.

The MH-Z19C sensor module has 6 pins: Ground, V_{in} , Pulse Width Modulation (PWM), Hd (for zero point calibration), along with Rx and Tx pins for data transfer. It has an operational voltage of 5.0 ± 0.1 , a peak current rating of 125mA and a CO₂ measurement range of 400 to 5000 PPM with an accuracy of ± 50 PPM + 5% of reading value [57].

2.2 Smart Classification to Determine Control Actions

In an automated hydroponics system, it is imperative to have a control system in place that determines the control action to be taken by the actuators of the systems in response to readings from sensors such that the optimal growth parameters for the plants can be maintained. Conventional automated hydroponics systems employ algorithms that use if-else conditional statements to pass along the control action to be taken to the actuators. Some systems, such as [58] and [59], have implemented smart classification algorithms to determine the control actions. These systems will be discussed in detail in the next chapter.

In our proposed system, we plan on implementing a novel approach to determine the control actions to be executed by the system. We will develop an XGBoost [60] classifier model for our system.

XGBoost, short for “Extreme Gradient Boosting”, is a highly optimized distributed gradient boosting library specifically designed to facilitate efficient and scalable training of machine learning models. It uses ensemble learning [61], a technique that combines the predictions of multiple individual models to create a more robust and accurate predictive model. XGBoost has garnered immense popularity and widespread utilization in the realm of machine learning, primarily due to its remarkable capabilities in handling extensive datasets and its capacity to attain state-of-the-art performance across various machine learning tasks, such as classification and regression.

One of the pivotal attributes of XGBoost lies in its adept handling of missing values, negating the need for extensive preprocessing when dealing with real-world data that often contains such gaps. Furthermore, XGBoost incorporates built-in support for parallel processing, a feature that expedites model training on substantial datasets. Furthermore, XGBoost exhibits high efficacy when dealing with tabular data with significantly lower training time as compared to deep training models [62].

The versatility of XGBoost is evident in its applications across a broad spectrum, encompassing arenas like Kaggle competitions, recommendation systems, and click-through rate prediction, among others. Its adaptability is further accentuated by the ease with which one can fine-tune various model parameters to optimize performance.

To comprehend XGBoost more comprehensively, it is imperative first to grasp the fundamentals of some techniques that add up to its ensemble learning approach.

1. Decision Tree: It is a structured flowchart where internal nodes signify attribute tests, branches represent test outcomes, and leaf nodes contain class labels. Trees are constructed by recursively partitioning the source data based on attribute tests until subsets with identical target variable values are achieved or when further splitting no longer augments prediction quality. Figure 2.9 illustrates the structure of a Decision Tree, starting from the root node up to the leaf nodes.

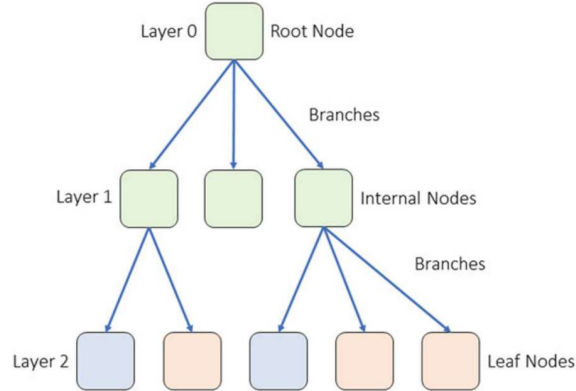


Figure 2.9: Illustrated example of a Decision Tree from the root node to leaf nodes [63]

2. Bagging: Short for Bootstrap Aggregating is an ensemble technique wherein base classifiers are trained on random subsets of the initial dataset. Individual predictions from these classifiers are then aggregated by voting or averaging to form a final prediction. Bagging mitigates overfitting by reducing variance but may introduce increased bias, offset by the variance reduction [63].

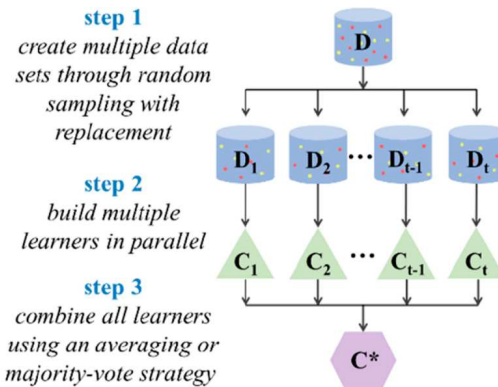


Figure 2.10: Illustration of bagging ensemble learning algorithm [64]

3. Random Forest: This ensemble method amalgamates multiple decision trees to lower variance. By combining their outputs through majority voting (for classification) or averaging (for regression), the resultant prediction benefits from the wisdom of the crowd. Random Forest incorporates bootstrap sampling to create diverse datasets for each model, thereby enhancing the overall robustness of the model [64].

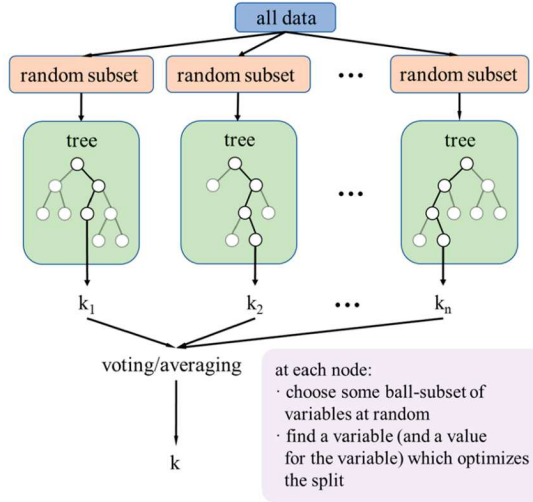


Figure 2.11: Illustration of the Random Forest algorithm [64]

4. Boosting: It is a distinct ensemble technique that aims to construct a robust classifier from numerous weak classifiers by sequentially building models. Each subsequent model endeavors to rectify the errors of its predecessor. This iterative process continues until the training data is either entirely predicted correctly or a predetermined limit on the number of models is reached.

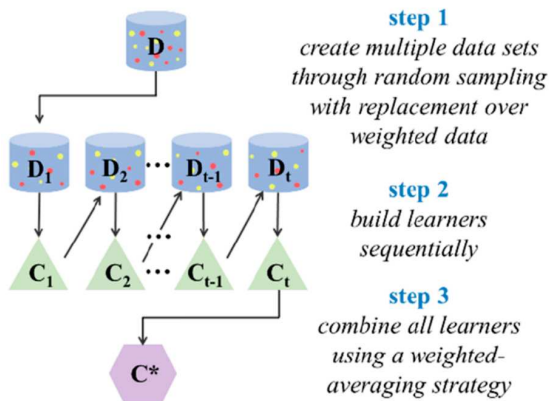


Figure 2.12: Illustration of the Boosting ensemble algorithm [64]

5. Gradient Boosting: It is a renowned boosting algorithm that propels each predictor to rectify the errors of the preceding one. Unlike Adaboost [65], which adds greater weight to the data points that are incorrectly classified for succeeding models, it does not manipulate the weights of training instances;

instead, each predictor is trained using the residual errors of the previous predictor as labels. The newer predictors are trained sequentially with errors from the previous predictor until the errors fall below the threshold margin. Within the realm of Gradient Boosting, a specific technique known as Gradient Boosted Trees employs CART (Classification And Regression Trees) as the base learner.

XGBoost, on the other hand, is an implementation of Gradient Boosted decision trees that sequentially employs decision trees, with the pivotal inclusion of weights assigned to independent variables. These weighted variables are fed into decision trees, and when inaccuracies arise, the weights of the incorrectly predicted variables are augmented before passing them to the subsequent decision tree. The amalgamation of these individual predictors yields a robust and precise model that can address regression, classification, ranking, and user-defined prediction challenges. Figure 2.13 shows an illustration of the XGBoost algorithm.

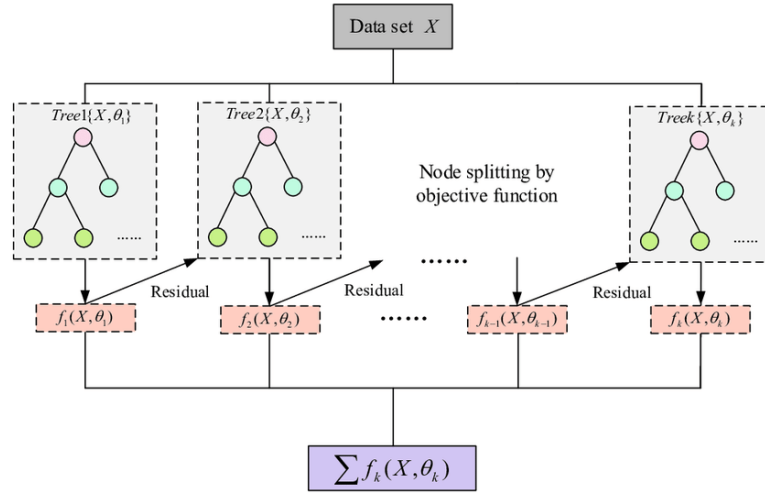


Figure 2.13: Illustration of the XGBoost algorithm [66]

2.3 Choice of Plant for The Proposed System

We chose lettuce (*Lactuca Sativa*) to test our system. With probable origins in Southern Europe and Western Asia [67], they are considered an excellent choice for hydroponics due to being easy to grow, the adaptability of their roots in nutrient-rich water, and their short growth period [68].

The optimal values for growth parameters for lettuce are given in Table 2.3:

| Electrical Conductivity (EC) of Nutrient Solution (microSiemens cm ⁻¹) | pH | Nutrient Solution Temperature (°C) | Air Temperature (°C) | | Light Intensity (mol m ⁻² d ⁻¹) | Dissolved Oxygen (DO) (mg L ⁻¹) | Humidity (%) | CO ₂ Concentration (Parts Per Million(PPM)) | |
|--|-----------|--|-------------------------|-------|---|---|-----------------|---|-------|
| | | | Day | Night | | | | Day | Night |
| 1100 - 1700 | 5.6 - 6.0 | 24 - 26 | 24 | 19 | 17 | 7 | 50 - 70 | 1500 | ~390 |

Table 2.3: Optimal Growth Parameter Values For Lettuce [69]

In our proposed system, an aerator is always used to aerate the nutrient solution such that the Dissolved Oxygen(DO) level does not fall below 7 PPM. Thus, we did not consider it a growth parameter that must be monitored and controlled rigorously as the others.

Chapter 3

Related Work

In this chapter, we highlighted some of the best works we came across during our literature review. Despite finding a large number of works pertaining to automated hydroponics, very few were published in reputable journals and conferences and were completely relevant to our proposed system. We discussed some of the most prominent works that we came across down below.

3.1 Automated Hydroponic Greenhouse [70]

D'Anna et al. [70] designed a small-scale automated IoT-enabled drip hydroponics system compact enough to fit inside regular-sized homes. Their system uses 4 different sensors (hygrometers, float sensors, temperature and humidity sensor array, pH sensor) to monitor:

1. Humidity
2. Air temperature
3. Moisture in the medium where the plants are placed
4. pH of the nutrient solution
5. Level of nutrient solution present in the growth channel

They controlled the light cycle by turning the LED array ON and OFF after regular intervals per the plants' specific requirements [71] and controlling the nutrients provided to the plants. A Raspberry Pi was used to take input from the sensors and control the actuators. A mobile app was developed to monitor the sensor readings or to start a new plant cycle while giving helpful information about handling and harvesting plants.

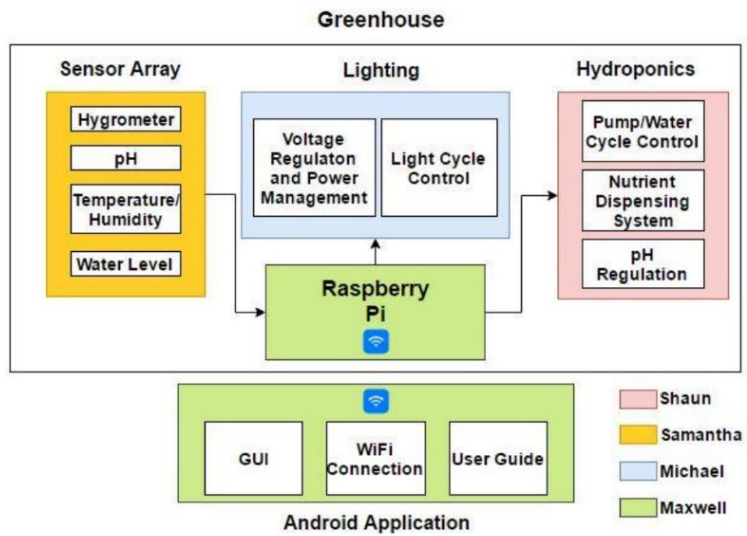


Figure 3.1: System Block Diagram [71]

3.1.1 Contributions

1. Provided detailed schematics and illustrations for the design of their system while mentioning the specifics of the hardware components used in their setup.
2. The mobile app is a positive source of agricultural information to users, especially those with little knowledge about the plants they want to grow.
3. The selection of LED arrays as the light source maximizes the usable energy for the plants, leading to greater overall system efficiency.

3.1.2 Limitations

1. Drip hydroponic systems are energy-inefficient, which offsets the gains in efficiency intended with their design
2. The water temperature and CO₂ concentration were neither measured nor controlled. If measured and controlled, the growth rate of the plants would have been significantly greater.

3.2 An Automated Hydroponics System Based on Mobile Application [72]

Kularbphettong et al. [72] designed and developed an automated IoT-enabled hydroponics system to introduce this modern agricultural practice to Thai farmers. Their study also included Functional Requirement, Functionality, Usability, Security, and Integrity tests for the system users to evaluate their satisfaction with how well their system works. Their system controls:

1. Humidity
2. Air temperature
3. Level of nutrient solution present in the growth channel

They made a Graphical User Interface (GUI) for the users to monitor the system remotely. The IoT system measured and recorded readings from the sensors on the server.

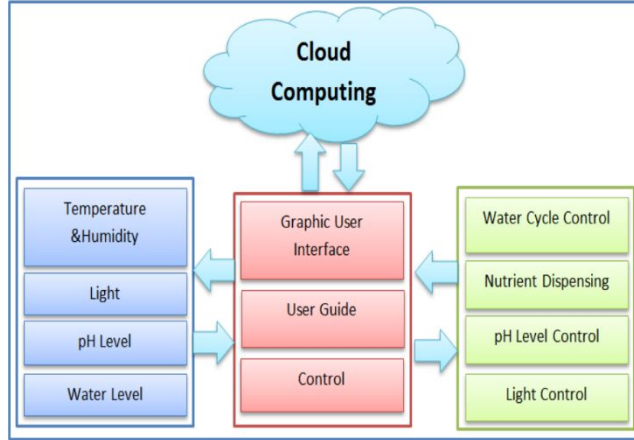


Figure 3.2: System Overview [72]

3.2.1 Contributions

1. The system's user-friendly design allows first-time users of hydroponic systems to use the system quickly.

3.2.2 Limitations

1. The system is rather minimalist regarding parameter control since it ignores nutrient concentration as well as CO₂ concentration. Since this work aims to introduce hydroponics to local farmers, this system does not provide the optimal conditions for the plants to grow at their highest possible rate.

3.3 Hydroponic Nutrient Control System based on Internet of Things and K-Nearest Neighbors [73]

Adidrana et al. [73] designed an automated IoT-enabled NFT system where they measured:

1. pH

2. Nutrient Concentration
3. Water temperature
4. Total Dissolved Solids (TDS) value

They then applied the k-Nearest Neighbor (KNN) algorithm [58], a supervised learning classifier, to predict the classification of nutrient conditions. The microcontroller takes the predicted results from the KNN algorithm. It sends commands to the actuator to vary the conditions of the nutrient solution and the system to maintain an optimal environment.

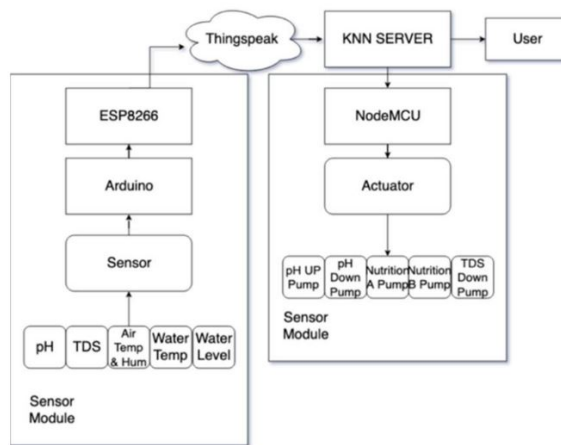


Figure 3.3: System Architecture [58]

3.3.1 Contributions

1. The application of KNN is a novel approach to making the decision-making process smart in automated hydroponics. This enables the system to decide what actions to take based on the data it collects from the sensors and reduces the need to program each case for which the conditions within the system must be altered via actuators.

3.3.2 Limitations

1. The air temperature, humidity, and CO₂ concentration were neither measured nor controlled. If measured and controlled, the growth rate of the plants would have been significantly greater.

3.4 Fully Automated Hydroponic System for Indoor Plant Growth [12]

3.4.1 Summary

Palande et al. [12] designed and developed an automated IoT-enabled hydroponics system to create a user-friendly system that can be used by anyone without requiring much technical knowledge. The parameters monitored by this system are:

1. pH
2. Air temperature
3. Water temperature
4. Humidity

They used two Arduino microcontrollers to take input from the sensors used in the system, which communicated with another Arduino which acts as the IoT network's gateway. The gateway Arduino communicates data to the Raspberry Pi, which handles the decision-making process to relay instructions to the actuators further to change the physical conditions within the system to maintain the ideal parameters for the growth of the plants.

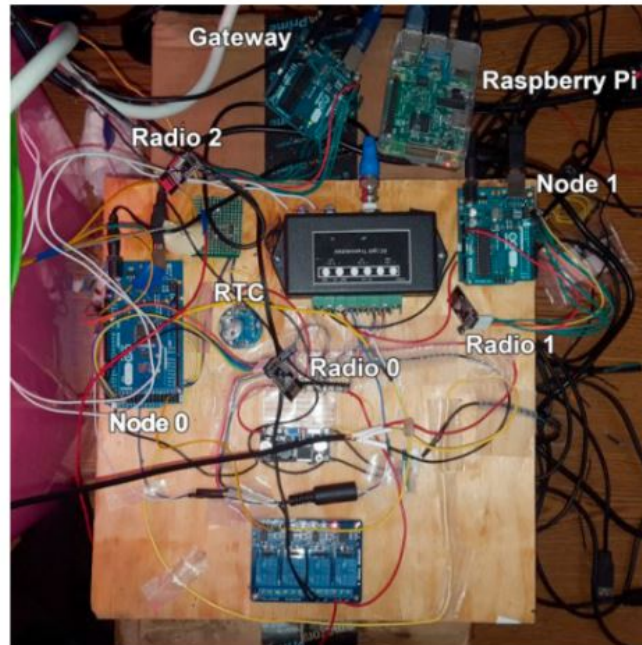


Figure 3.4: Hardware components of the system [12]

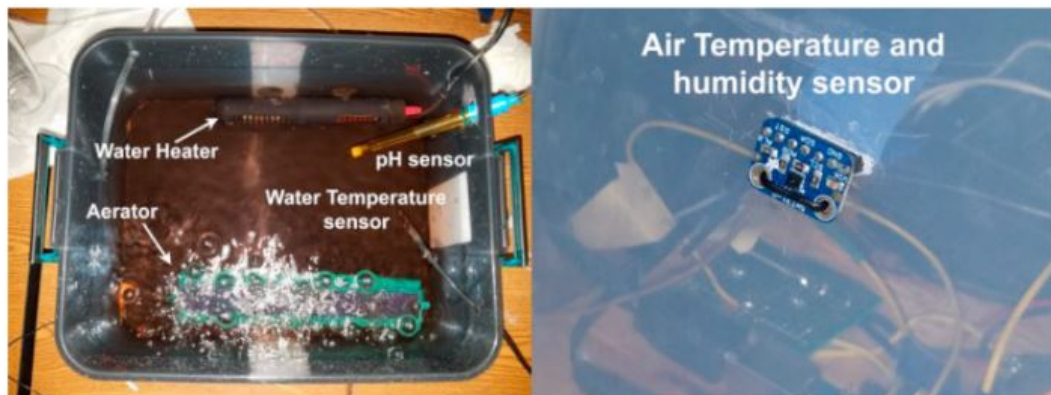


Figure 3.5: Different sensors and parameter inducers [12]

3.4.2 Contributions

1. Implementing Arduinos as nodes to handle data from sensors reduces the chances of total system failure since any errors in the sensors would not affect the function of the Raspberry Pi; it would still transmit messages to the mobile app.

3.4.3 Limitations

1. The nutrient concentration, CO₂ concentration, and light intensity were neither measured nor controlled. If measured and controlled, the growth rate of the plants would have been significantly greater.

3.5 The Design and Implementation of a Hydroponics Control System [74]

Griffiths et al. [74] designed and built an automated hydroponic system to grow produce easily and cheaply. This system monitors:

1. pH
2. Nutrient Concentration
3. Water temperature
4. Light Cycle

The work goes into great detail on the design and construction of the system, with an extensive focus on the GUI.

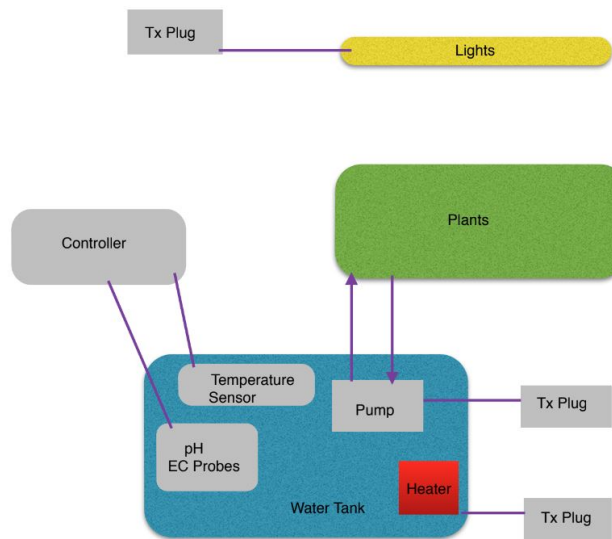


Figure 3.6: Overall view of the system [74]

3.5.1 Contributions

1. The work discusses the system's design and implementation expansively. The development of the Printed Circuit Board (PCB) to house the electronics added to the compact nature of the system.
2. The comprehensive GUI allows users to monitor and control the system better than most conventional IoT-enabled automated hydroponics systems.

3.5.2 Limitations

1. The system was not tested to see how plants would grow, which questions the system's reliability in getting the desired results.
2. The nutrient concentration, CO₂ concentration, and air temperature were neither measured nor controlled. If measured and controlled, the growth rate of the plants would have been significantly greater.

3.6 IoT based hydroponics system using Deep Neural Networks [59]

Mehra et al. [59] designed and developed an intelligent IoT-enabled hydroponics system that uses deep neural networks to determine the control actions required to adjust the physical conditions within the growth space of the system where the team grew tomatoes. This system monitors:

1. Humidity
2. Water Level
3. Light Intensity

The system was designed to take readings from the system using sensors that send the data over to the microcontroller, which transfers the data to the Raspberry Pi 3. The deep neural network model is loaded onto the Raspberry Pi 3, which uses the sensor readings to predict the control action needed.

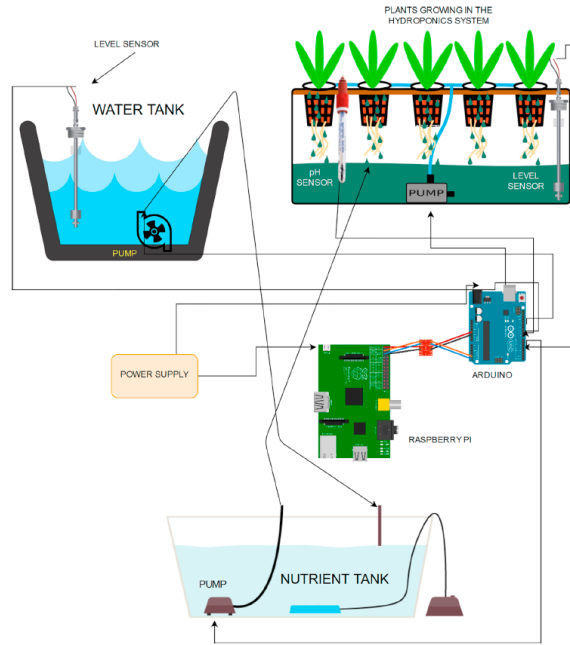


Figure 3.7: System architecture of IoT based hydroponics [59]

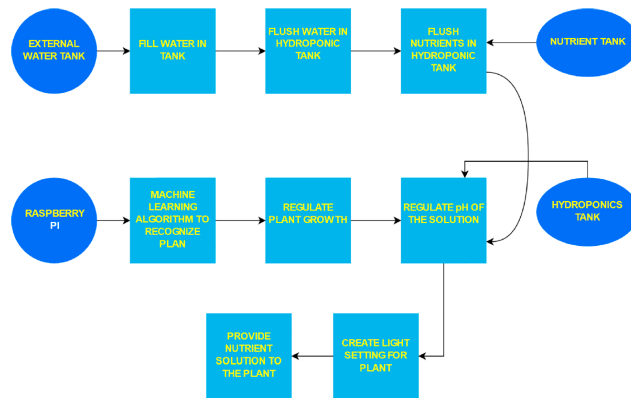


Figure 3.8: Data flow diagram [59]

3.6.1 Contributions

1. The implementation of deep neural networks for the decision making mechanism of the system is novel. This goes to show the possible scope of implementing such smart algorithms in decision making systems.
2. Using the Arduino microcontroller and Raspberry Pi 3 as independent controllers mitigates the changes of total system failure in the event that one of them malfunctions.
3. The study compared the height of the tomato plants which were grown inside the hydroponics system with a control group of tomato plants which were grown in soil using conventional methods.

3.6.2 Limitations

1. The system was designed to control only humidity, water level and light intensity. While air temperature and TDS were monitored, the system was not equipped to control those parameters. The system did not monitor nor control CO₂ concentration.
2. The method of defining control actions is inefficient. If the system is scaled to control more growth parameters, then defining the control actions in the same manner would lead to a large number of unique control actions which would make programming the microcontroller and actuators significantly complicated and difficult.

3.7 Automated system developed to control pH and concentration of nutrient solution evaluated in hydroponic lettuce production [75]

3.7.1 Summary

Domingues et al. [75] designed and developed an automated hydroponics system specifically to grow lettuce. They proposed their system as an alternative means for the mainstream agricultural production of lettuce. The system monitors and controls:

1. pH
2. Electrical Conductivity
3. Water Temperature

They developed their own software to monitor and control the hydroponics system named ControlHidro. Their proprietary software monitored the two parameters 24h throughout the growth cycle of the lettuce. The pH and EC were controlled by means of adding additional acid, base and nutrients to the nutrient solution by actuating 2-way solenoid valves as seen in Figure 3.9.

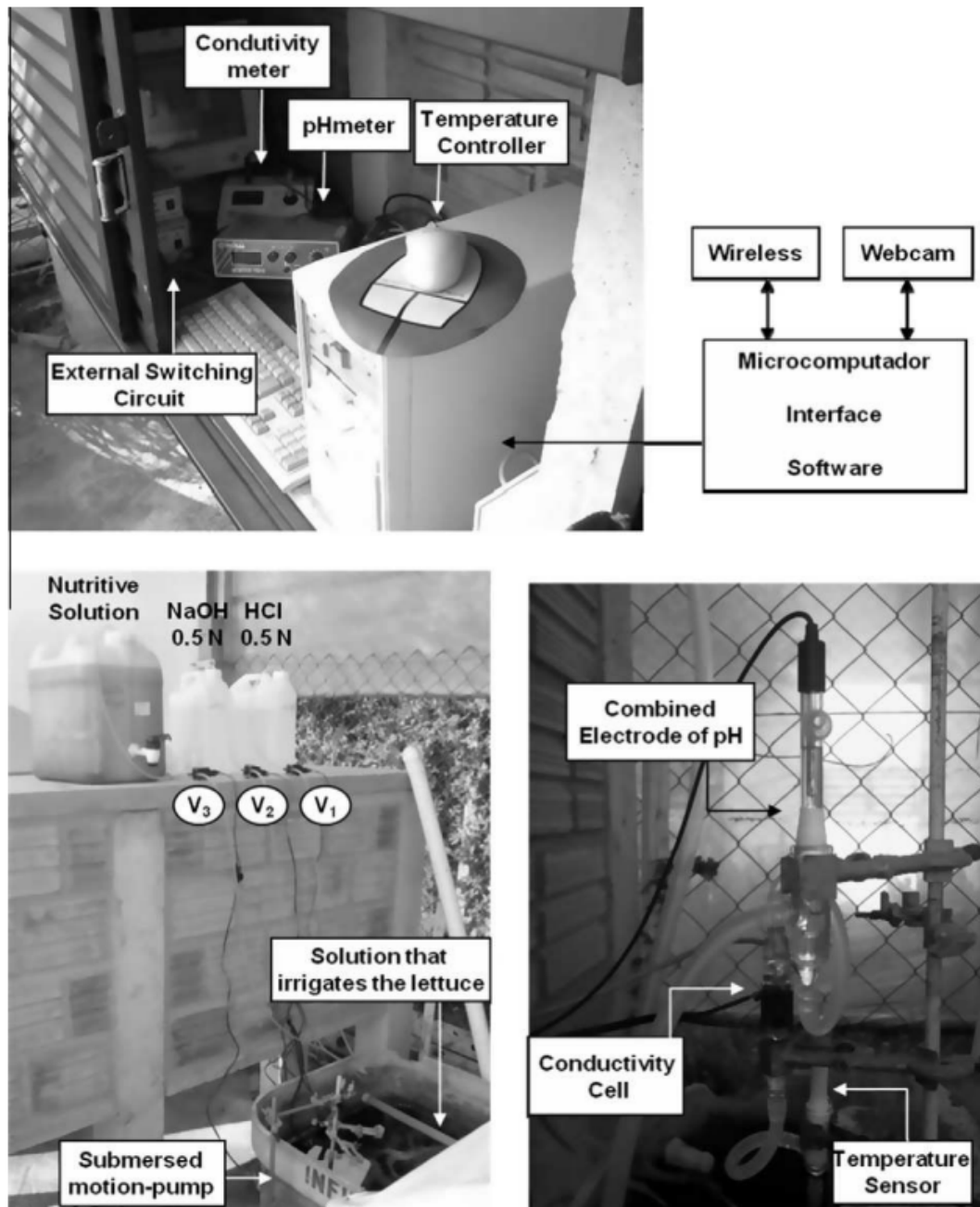


Figure 3.9: Flowchart of instrumental system developed by DIA/UEL Group, utilized in monitoring and control of hydroponic lettuce. V1, V2 and V3 are solenoid valves [75]

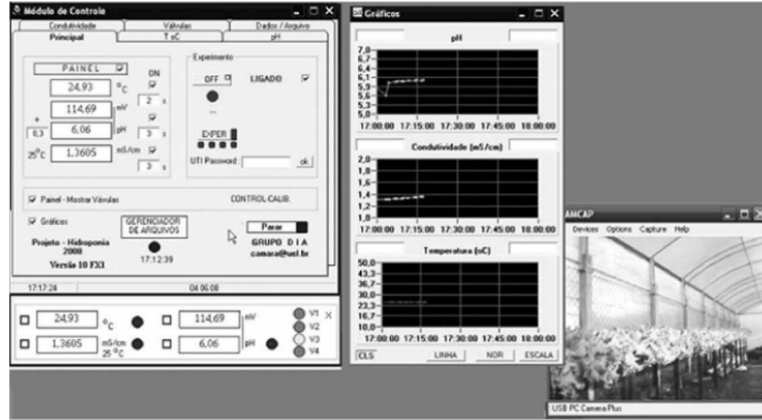


Figure 3.10: Digitized screen of software ControlHidro and image of automated hydroponic cultivation obtained through a webcam by remote connection [75]

3.7.2 Contributions

1. The development of a system focused towards the production of lettuce allowed them to benchmark the system against previous systems designed for hydroponically grown lettuce. Their system resulted in a significant improvement in the growth markers for lettuce, such as average of fresh mass of aerial part (FMAP), average of dry mass of aerial part (DMAP), dry root mass (DRM), total number of leaves (NTF) and leaves higher than ten centimeters (NF10).
2. They developed their own software to monitor the pH and EC. This gave them a good degree of flexibility in the design of the system as they could easily interface their software to the sensors and actuators per their requirements.

3.7.3 Limitations

1. They did not monitor or control humidity, CO₂ concentration, light intensity and air temperature.

3.8 Observations from Related Works and Conclusion

In an automated hydroponics system, the seven key parameters contributing the most towards the growth of the plants are nutrient concentration, pH, CO₂ concentration, water temperature, air temperature, humidity, and light cycle/intensity. None of the works discussed has developed a system where all the parameters are monitored and controlled smartly.

Table 3.1 below compares the works mentioned earlier to illustrate the limitations of those works.

| Cited Works | Parameters monitored and controlled | | | | | | | | |
|-----------------|-------------------------------------|----|-----------------|-----------------|-------------------|----------|---------------------------|-------------|--|
| | pH | EC | CO ₂ | Air Temperature | Water Temperature | Humidity | Light Intensity/ Cycle | Water Level | |
| [70] | ✓ | X | X | ✓ | X | ✓ | X | ✓ | |
| [72] | X | X | X | ✓ | X | ✓ | X | ✓ | |
| [73] | ✓ | ✓ | X | X | ✓ | X | X | X | |
| [12] | ✓ | X | X | ✓ | ✓ | ✓ | X | X | |
| [74] | ✓ | ✓ | X | X | ✓ | X | ✓ | X | |
| [59] | X | X | X | X | X | ✓ | ✓ | ✓ | |
| [75] | ✓ | ✓ | X | X | ✓ | X | X | X | |
| Proposed system | ✓ | ✓ | ✓ | ✓ | ✓ | ✓ | ✓ | ✓ | |

Table 3.1: Tabular comparison of the related works

From Table 3.1, it can be seen that there are substantial limitations in all previous works. In comparison, our proposed system, which is highlighted, aims to monitor and control all of the parameters, as seen in the last row of the table.

Furthermore, none of the systems measured or controlled the level of CO₂ present in the system. Most of the works focused on parameters that were relatively easy to monitor, such as water and air temperature, pH, humidity, and nutrient concentration. Some works, such as [12], have designed the system to control water temperature, which was mainly only measured in most systems.

Additionally, all the works mentioned are single-growth unit systems, accommodating one species of plants during one growth period.

Lastly, the IoT implementation of the systems aims at only providing a means of monitoring the system's physical state while not leaving much for the user to control remotely. In addition, implementing intelligent decision-making algorithms in these automated systems, such as in [73], is likely to make the system much less reliant on user supervision. The need to implement any possible cases within the system is eliminated with such implementations of intelligent algorithms.

Our proposed system is designed to address these limitations of previous works as well as build upon their strengths and output.

Chapter 4

Methodology

A traditional NFT hydroponics system comprises mainly two sections: the growth channels, which are placed at an elevation, and the reservoir below it[5] as shown in Fig. 1.1 The electric pump pushes nutrient solution up into the growth channels, where the plant roots come in contact with the solution. The solution then moves down the slope of the channels and back to the reservoir.

4.1 Proposed System

4.1.1 System Modules

We based our design on the NFT hydroponic system in our proposed system. It will be a closed hydroponics system that can monitor and control the key physical parameters required by a plant to grow optimally, thus accelerating its growth rate and eliminating the need for pesticides. The system can have multiple units where the plants are grown, called Growth Modules(GMs).

Each of these GM modules can be used to produce the same plant or different species. The entire system will have its physical parameters independently monitored by sensors connected to an Arduino Nano. The Nano will transmit the signals to the Raspberry Pi 4, which will also host the central server for the system. The Pi will decide the control action to be taken by the actuators and then

send signals to the Arduino Mega connected to the actuators. The Mega then controls the actuators to regulate the physical parameters within the system. The Nutrient Solution Container Module(NSCM) will supply the GM with nutrient solution per the plant's needs. The NSCM will maintain the nutrient solution at the optimal temperature, pH, and concentration and adjust it according to the needs of the plants in the GMs.

Figure 4.1 illustrates how the GM and NSCM interact to maintain a constant flow of nutrient solution between them to supply the plants with nutrients while maintaining the nutrient solution at uniform conditions.

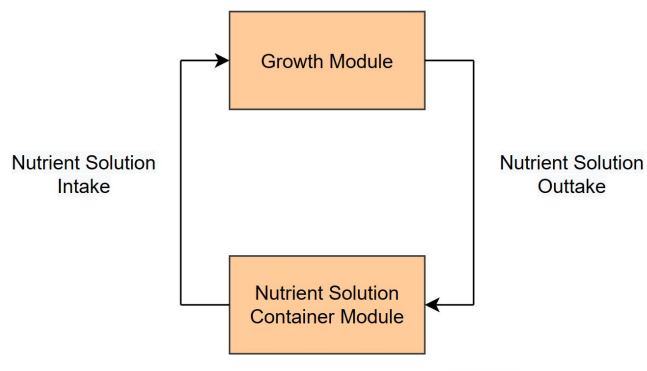


Figure 4.1: Simplified outline of the system

The details of the modules are as follows:

1. Nutrient Solution Container Module:

This module will hold the nutrient solution to be used in our system. The nutrient solution will mainly constitute Nitrogen(N), Phosphorus(P), and Potassium(K), with the addition of a multitude of other nutrients as mentioned in Tables 2.1 and 2.2, depending on the type of plant we would like to grow. Figure 4.2 below shows a block diagram listing all the sensors and actuators this module will use.

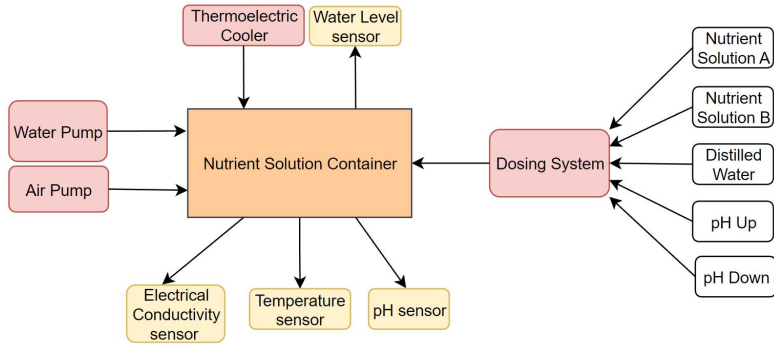


Figure 4.2: Block diagram for the Nutrient Solution Container Module

As can be seen in Figure 4.2:

- (a) The pH sensor will constantly measure the pH level of the nutrient solution in the container. If the pH level is outside the optimal pH range required for the specific plant type, the dosing system adds acid or base to the nutrient solution to bring the pH back within the optimal range.
- (b) A Water level sensor will measure the height at which the nutrient solution is present to determine the amount of nutrient solution within the system. If the height of the nutrient solution falls or exceeds drastically, the central server will issue a warning.
- (c) A Electrical Conductivity (EC) sensor will measure the concentration of nutrient ions in the solution if the EC reading is outside the optimal EC range required for the specific plant type. In that case, the dosing system adds a concentrated nutrient solution or distilled water to the nutrient solution to bring the EC readings back within the optimal range.
- (d) A temperature sensor will measure the ambient air temperature within the module. The thermoelectric cooler can return the temperature to the desired level if the temperature rises and exceeds the optimal temperature range.
- (e) An air pump will oxygenate the solution and help the dissolved nutrients mix evenly throughout the solution. It will always be running to ensure that the Dissolved Oxygen (DO) remains above the required level.

- (f) A water pump will constantly pump the nutrient solution to the GMs as it returns to the NSCM, creating a non-stop flow of nutrient solution, ensuring that the plant roots receive a constant supply of water, dissolved oxygen, and nutrients.

2. Growth Module:

This is the module where the plants will be grown. Figure 4.3 illustrates a block diagram of the sensors and actuators being used in the Growth Module.

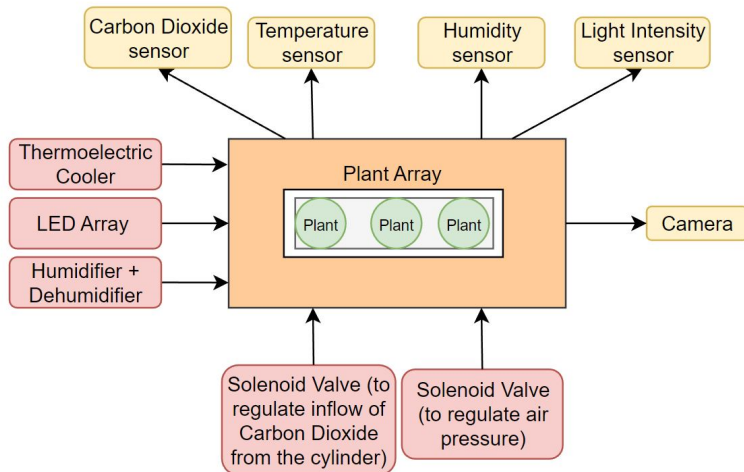


Figure 4.3: Block diagram for the Growth Module

From Figure 4.3, the mechanism with our proposed GM will work as follows:

- A temperature sensor will measure the ambient air temperature within the module. The thermoelectric cooler can return the temperature to the desired level if the temperature rises and exceeds the optimal temperature range.
- A humidity sensor will measure the humidity inside the Growth Module. If there is a change in the optimal humidity percentage, the humidifier or dehumidifier will be actuated to bring the humidity back to the optimal range.
- An on-off solenoid valve will regulate the air pressure and CO₂ concentration inside the growth module. The exhaust from the system will be

fed into a CO₂ scrubber, which will remove CO₂ gas before the air returns to the surrounding environment, mitigating the risk of fatal CO₂ build-up in the location where the system will be used.

- (d) A Carbon Dioxide (CO₂) sensor will monitor the concentration of CO₂ gas within the system. Suppose the concentration falls or exceeds the optimal range. In that case, an on-off solenoid valve will be actuated to allow the inflow of CO₂ gas into the system to bring the concentration within the optimal range.
- (e) A thermoelectric cooler will work in response to the temperature sensor readings; if there is a change in the optimal temperature, then the thermoelectric cooler will be actuated to bring the temperature back to the optimal range.
- (f) A light intensity sensor will constantly measure the light intensity level inside the Growth Module. The LED arrays are turned ON and OFF for a set duration to ensure that the plants receive light for an extended period while also getting adequate downtime to allow for healthy growth.
- (g) A camera will be used to provide a constant video feed of the interior of the Growth Module. This will allow us to see how well the plants are growing. We will also deploy a Machine Learning model to monitor the growth of the plants.

4.1.2 IoT Environment

Once assembled and connected, the GMs and NSCM will be connected to a Raspberry Pi 3. The environment for the system, as well as the IoT framework, is illustrated below in Figure 4.4.

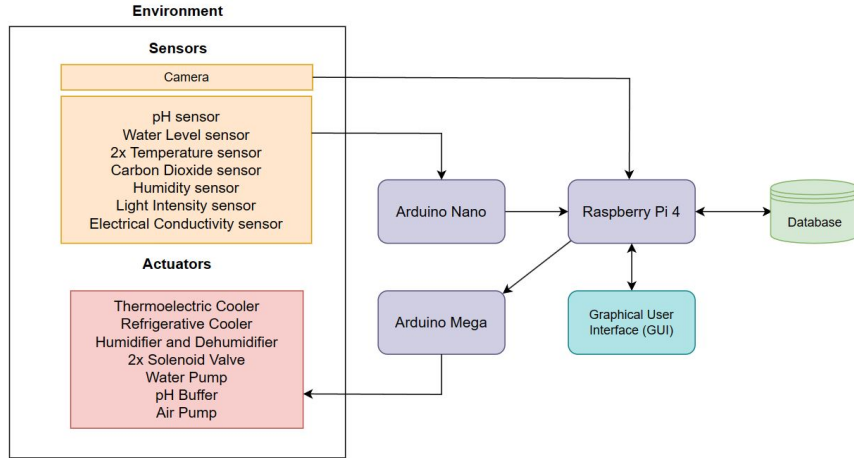


Figure 4.4: Block diagram for the IoT framework of the system

The readings from the sensors in the GMs and NSCM will be transmitted to Arduino Nanos, which in turn send the signals to the Raspberry Pi.

The Raspberry Pi will apply an intelligent classification algorithm based on the sensor data collected over time to determine the appropriate control actions whenever the system requires it. The control action signals for the actuators are transmitted to the Arduino Megas, which then send the signals to the actuators in the modules.

This approach to using Arduinos as nodes is inspired by [12]. Transmitting signals between the Raspberry Pi, Arduino Nanos, and Megas creates a safety net. The Raspberry Pi will remain fully operational if a sensor, actuator, or module malfunctions. This will allow us to quickly identify which components of the modules are acting anomalously and identify the error without compromising the entire system.

Figure 4.5 illustrates the connectivity between the Arduino microcontrollers of the modules with the Raspberry Pi.

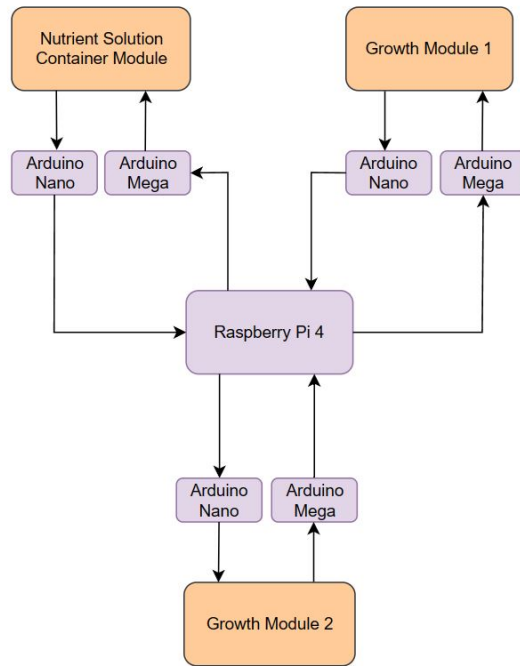


Figure 4.5: Block diagram for communication between the Arduino microcontrollers and the Raspberry Pi

Figure 4.6 shows a flow diagram to illustrate the entire system.

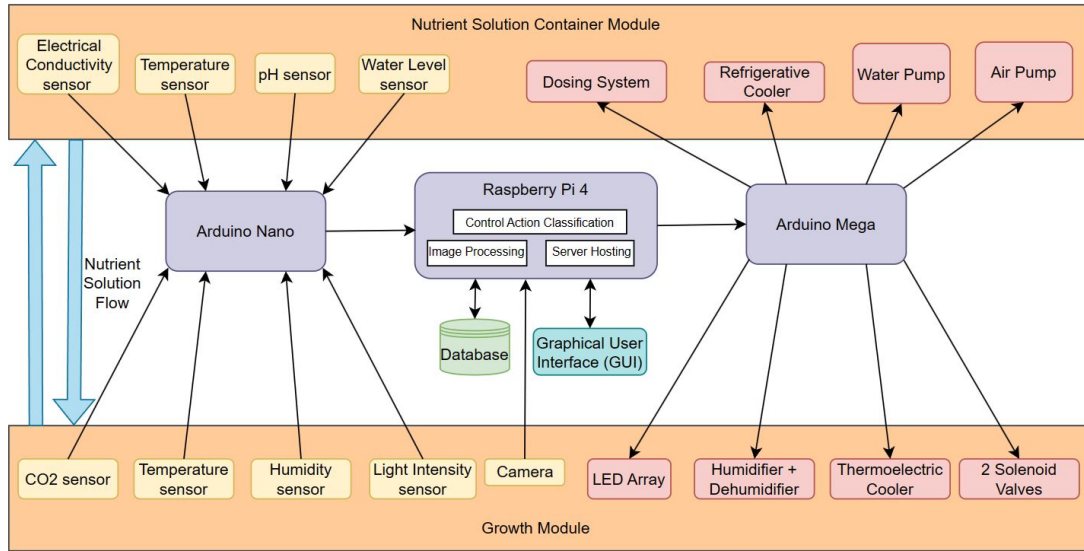


Figure 4.6: Flow diagram for the entire system

4.2 Implementation of Proposed System

We started the work by developing a 3D CAD model of a traditional NFT hydroponic system. The designing phase of the 3D model allowed us to visualize the type of system we have proposed and wish to develop, leading us to design a slightly modified NFT hydroponic system.

4.2.1 3D CAD Model

Figure 4.7 shows the 3D CAD model we developed for our proposed system from different views. The model was developed using SOLIDWORKS 2018.

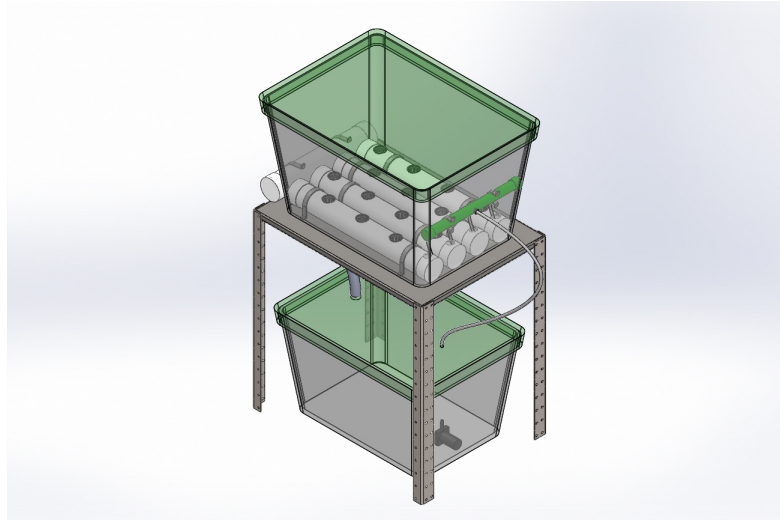


Figure 4.7: Overhead view of the 3D CAD model of the system

Our intention for the proposed system is to make it as compact as possible while ensuring we can attach the required sensors, actuators, and controllers to the modules.

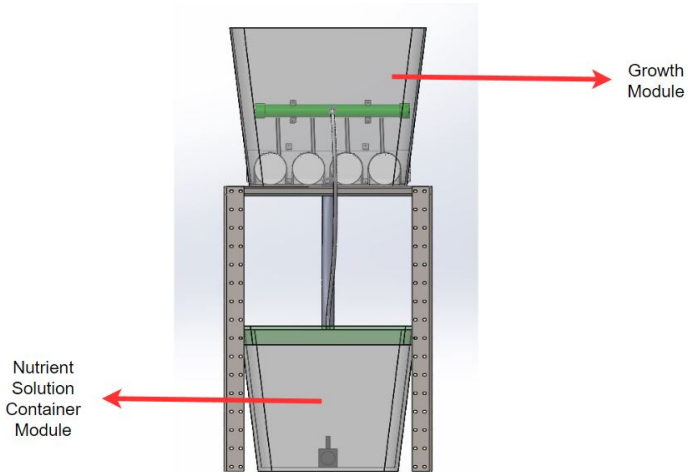


Figure 4.8: Left view of the 3D CAD model of the system

Figure 4.8 shows our Nutrient Solution Container Module (NSCM) and Growth Module (GM) labeled. We kept the two modules at a vertical height from each other to allow for smooth pumping action by the water pump, which is discussed at length below.

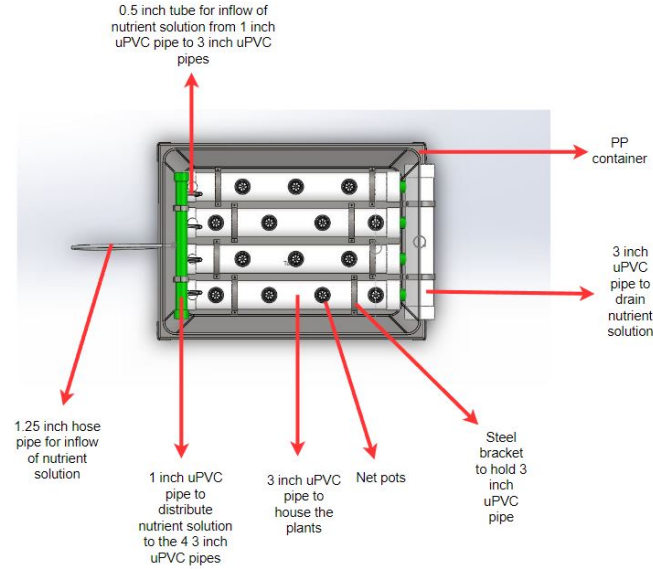


Figure 4.9: Top view of the 3D CAD model of the system

Figure 4.9 shows the system from a top view. Our design is based on the NFT system. Thus we adopted to make growth channels out of 3-inch uPVC pipes where the net pots meant to house the plants are placed 6 inches from each other [76].

While designing the system, we realized that using 0.5-inch silicone tubes to distribute nutrient solution from the 1-inch uPVC pipe was a better choice due to the low flow rate that went into each 3-inch uPVC pipe.

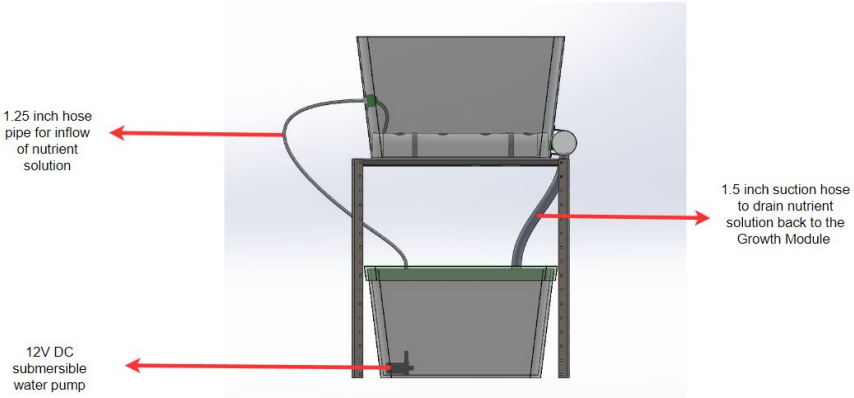


Figure 4.10: Front view of the 3D CAD model of the system

Figure 4.10 shows the system's overall nutrient solution pumping mechanism. The nutrient solution is pumped into the 1.25-inch hose pipe by the 12V DC submersible water pump. After flowing its course through the 1-inch uPVC, it is distributed to the four 3-inch uPVC pipes via the 0.5-inch silicone tubes. The design was made such that after being in contact with the roots of the plants, the nutrient solution from the four 3-inch pipes is collected in the other 3-inch uPVC pipe mounted on the side, as seen in Figure 4.9.

Figure 4.11 shows the right view of the system, where the 3-inch uPVC pipe where the nutrient solution flows to be drained can be seen. A 1.5-inch threaded nipple makes the opening in the 3-inch uPVC pipe at a height from the lowest point in the pipe. This causes the nutrient solution to accumulate in the 3-inch uPVC pipe, giving ample time for the roots to receive dissolved oxygen and nutrients. This differs from traditional NFT systems where the “film” of nutrient solution is thin at around 5mm in height. In comparison, the height of the nutrient solution inside the 3-inch uPVC pipes is approximately 25mm.

This aspect of the design allows the nutrient solution to collect into a larger pipe before going back down to the NSCM, preventing any form of overflow within the system.

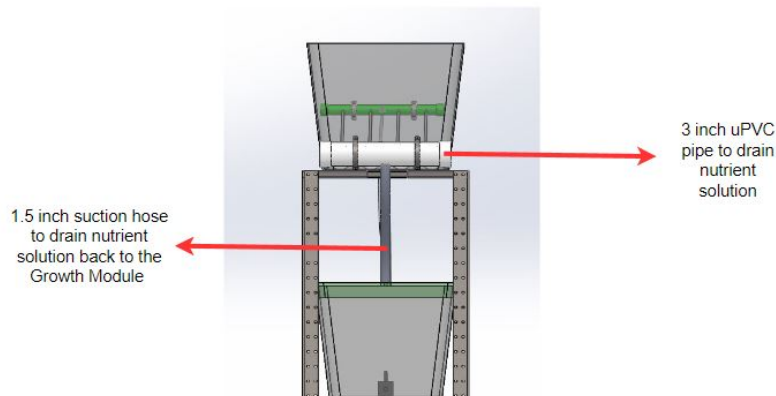


Figure 4.11: Right view of the 3D CAD model of the system

Figure 4.11 shows the 3-inch uPVC pipe mounted at the side of the GM to collect the nutrient solution. After the nutrient solution drains into the 3-inch uPVC pipe, its flow rate is very low, making it difficult to pass it through flexible tubing and

regular hose pipes. This led us to use a 1.5-inch suction hose to design this system, which can maintain a rigid frame and constant circular diameter throughout its length to allow the nutrient solution to flow back into the NSCM with the help of gravity.

Sensor holders were designed to hold the sensors in place in the NSCM, as shown in Figures 4.12, 4.13, 4.15 and 4.14. These holders, designed to be fitted with nut and bolts, are mounted on a 0.75-inch uPVC pipe attached width-wise to the NSCM. The sensor holders are designed to hold the sensors at adjustable heights, allowing the system to have the flexibility to vary the height of nutrient solution in the NSCM as required. The sensor holders are designed to hold the pH probe, temperature probe, TDS probe and ultrasonic sensor, which measure the height of nutrient solution in the NSCM.

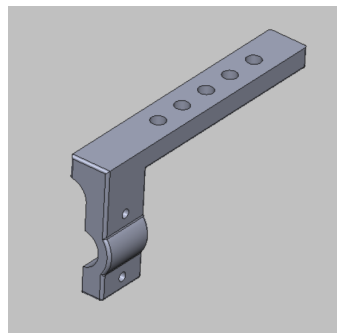


Figure 4.12: 3D model of pH probe holder clamp

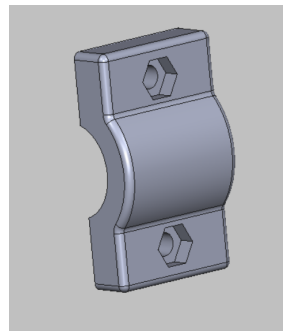


Figure 4.13: 3D model of pH probe holder clamp head

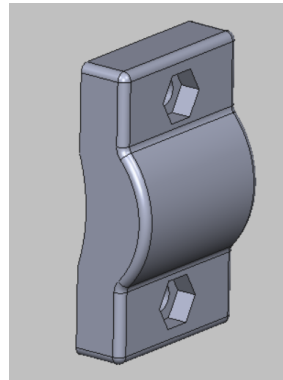


Figure 4.14: 3D model of pH probe holder clamp head

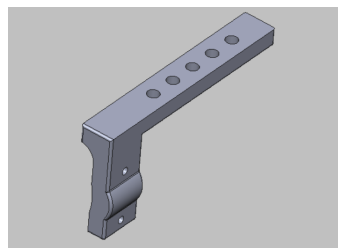


Figure 4.15: 3D model of EC probe holder clamp

4.2.2 Physical Structure

Per the design, we developed a physical system based on two polypropylene (PP) containers using which we built the GM and NSCM. The plants will be placed in net pots housed inside circular incisions, 6 inches apart [76], inside 3-inch uPVC pipes, as seen in Figure 4.16.

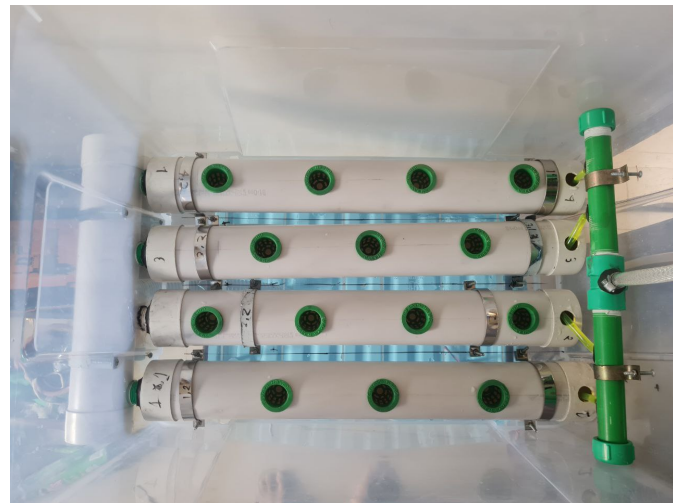


Figure 4.16: Top view of the physical structure

The 3-inch pipes are held in place by steel brackets as the system can hold a total of 14 plants per growth cycle, as seen in Figure 4.16. The 1.5-inch hose pipe brings up nutrient solution pumped up by the 12V DC submersible water pump, as seen in Figure 4.17 below, from the GM, which is then sent to the 1-inch to be distributed to the 4 3-inch pipes.



Figure 4.17: Front view of the physical structure

After flowing along the 3-inch pipes and being in contact with the roots of the plants, the nutrient solution gathers in the 3-inch uPVC pipe and flows down to the NSCM via the 1.5-inch suction hose as seen below in Figure 4.18 down below.

The process keeps repeating as nutrients are steadily supplied to the roots of the plants being grown in the GM.



Figure 4.18: Right view of the physical structure



Figure 4.19: Water flowing from the 3-inch uPVC pipe back to the NSCM via the 1.5-inch suction hose

Figure 4.19 shows that the nutrient solution flows back into the NSCM after being collected in the 3-inch uPVC pipe via the 1.5-inch suction hose. This results in the constant re-circulation of the nutrient solution throughout the system, ensuring a steady supply of nutrients to the plants throughout their growth cycle.

The sensor holders are 3D printed using Acrylonitrile Butadiene Styrene or ABS plastic and fitted using steel bolts and nuts. Figure 4.20 shows the temperature

probe, pH probe, TDS probe and ultrasonic sensors being held in place with the holders at a height above the nutrient solution such that all the probes were fully submerged at all times.

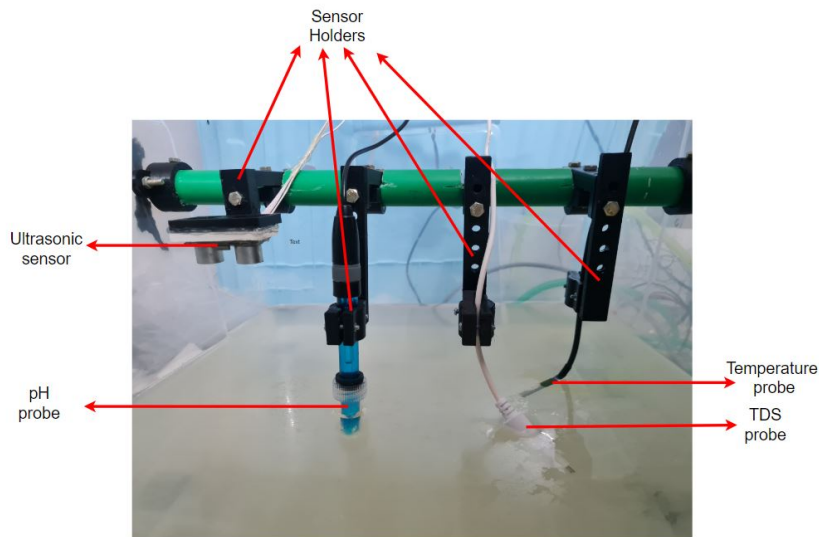


Figure 4.20: Ultrasonic sensor, pH probe, TDS probe and temperature probe held above the nutrient solution by the sensor holders

4.2.3 Sensors

4.2.3.1 Initial Approach of Calibration and Placement of a Low-end pH Sensor

The Atlas Scientific pH Kit had to be brought in from overseas and had a wait time for its delivery, which left us with no alternative but to use a locally available, low-end pH sensor kit.

Due to the analog nature of this low-end pH sensor, it required calibration, and this probe is designed to have a linear calibration graph [77]. We used pH buffer solutions of three different pH values: 4.00, 6.86, and 9.19. The pH probe was immersed into the three pH buffer solutions. We determined the settling time for the voltage readings on the pH probe to be between 2 to 3 minutes. Before this time, the voltage readings are subjected to overshoots and mild fluctuations. Taking 3 minutes as the standard settling time, we took readings of the voltages produced across the two electrodes of the pH probe from the Serial Monitor of the

Arduino. The corresponding voltage readings from the three pH buffer solutions are given in Table 4.1.

| pH | Voltage Reading (V) |
|------|---------------------|
| 4.00 | 1.56 |
| 6.86 | 2.17 |
| 9.19 | 2.70 |

Table 4.1: Voltage readings from pH probe calibration with buffer solutions of pH 4.00, 6.86, and 9.19

The three data points were used to make a scatterplot using Seaborn, a Python data visualization library based on the more popularly used matplotlib library, which can be seen in Figure 4.21. Linear regression is applied to the scatterplot to obtain the equation relating the pH of the solution in which the pH probe is submerged to the voltage produced across its electrodes.

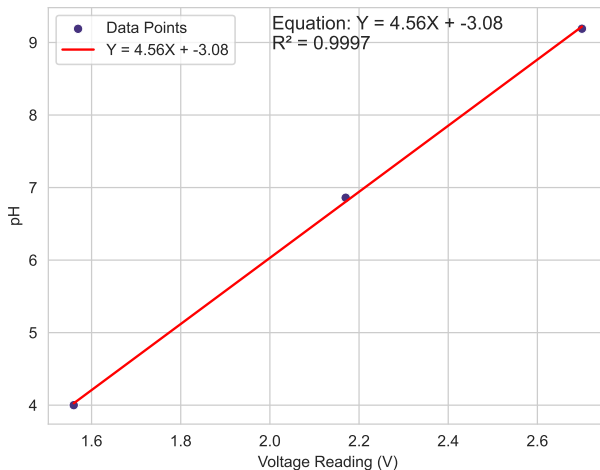


Figure 4.21: Scatter-plot of pH against electrode voltage graph, plotted in Seaborn

The equation for the pH readings is determined to be:

$$y = 4.56x - 3.08 \quad (4.1)$$

y is the pH of the solution, and x is the voltage produced across the electrodes in the pH probe in Volt(V). Equation 4.1 has an R-squared value of 0.9997, indicating an excellent fit for the three data points. Thus, this equation was used by the Arduino Nano to calculate the pH from the voltage produced at the electrodes. The probe has a measuring accuracy of ± 0.1 with an operating voltage of 3.0 to 5.5V [78].

The pH probe is held by the sensor holder, as seen in Figure 4.20, such that its tip is entirely submerged in the nutrient solution to monitor the pH of the solution. The sampling rate of the pH sensor is set at 0.05 readings every second or 1 reading every 3 minutes to allow the probe reading to settle.

4.2.3.2 Current Approach of Using the Atlas Scientific pH Kit

As we kept running our system and testing the sensors and actuators, we noticed that the readings of the low-end pH sensor started to drift even when nothing was added to the nutrient solution. Upon investigation, we learned that this pH probe is unsuitable for being immersed indefinitely in a solution as it quickly loses its calibration and requires frequent calibration. As much as once every 5-6 hours.

As such, this sensor is unsuitable for our system, which would require the probe to be immersed indefinitely in the nutrient solution. This led us to use the Atlas Scientific pH Kit. Compared to the low-end pH sensor, the Atlas Scientific pH Kit probe could be immersed indefinitely in the nutrient solution and only required calibration once every 6 months. The Atlas Scientific pH Kit also has a more straightforward calibration process:

1. The probe is immersed into one of the 3 pH buffer solutions provided at pH 4.00, 7.00, and 10.00. The probe is connected to the signal conversion circuit board, which uses the Universal Asynchronous Receiver-Transmitter(UART) protocol to send the data to the Arduino Nano.

2. The Serial Monitor monitors the data received by the probe. The initial readings are off by a significant margin as they start to settle closer to the actual pH of the buffer solution.
3. Once the fluctuations in readings go down, the command “Cal,L,X” is sent to the sensor via the Serial Monitor, where L is the level of the point, which can be high, medium, or low on the calibration graph. X is the value of the pH of the buffer solution. Table 4.2 below lists the 3 commands sent via the Serial Monitor for the 3-point calibration.

| pH | Calibration Command |
|-------|---------------------|
| 10.00 | Cal,high,10.00 |
| 7.00 | Cal,mid,7.00 |
| 3.00 | Cal,low,4.00 |

Table 4.2: List of calibration commands sent to the Atlas Scientific pH Kit

4. Upon sending the correct calibration command, the Serial Monitor responds with an “*OK” message, indicating that the single-point calibration was completed without any errors. The probe is then gently removed from the buffer solution and cleaned using distilled water.
5. The 3-point calibration is finished by repeating steps 1 through 4 for all 3 of the pH buffer solutions. To check whether the overall calibration process succeeded, the pH probe is immersed into a different pH buffer solution of pH 6.86. After a settling time of approximately 10 seconds, the sensor gave a reading of 6.85. This indicated that the calibration process was completed without any errors.

The low-end pH sensor is replaced by the Atlas Scientific pH sensor and is held by the sensor holder, as seen in Figure 4.22, such that its tip is entirely submerged in the nutrient solution to monitor the pH of the solution. The sampling rate of the pH sensor is set at 0.05 readings every second or 1 reading every 3 minutes to allow any changes made to the pH of the nutrient solution by the dosing system to take full effect from mixing.

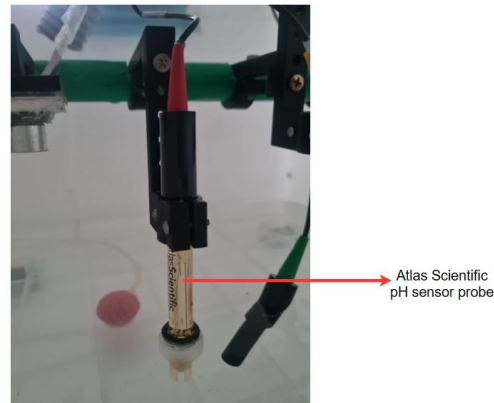


Figure 4.22: Atlas Scientific pH sensor probe fixed on the sensor holder and immersed in nutrient solution

4.2.3.3 Placement of Air Temperature and Humidity Sensor

The DHT22 sensor is placed inside the GM, as seen in Figure 4.23, so the sensor is constantly exposed to the ambient air inside the GM. The sampling rate of the DHT22 sensor is set at 0.05 readings every second or 1 reading every 3 minutes. This is done to allow the readings of air temperature, humidity, and pH to be taken synchronously.



Figure 4.23: DHT22 sensor mounted on the side wall of the Growth Module

4.2.3.4 Placement of Water Temperature Sensor

The DS18B20 Digital temperature sensor probe is held by the sensor holder, as seen in Figure 4.20, such that its tip is entirely submerged in the nutrient solution to monitor the temperature of the solution. The sampling rate of the pH sensor is set at 0.05 readings every second or 1 reading every 3 minutes. This is done to allow the readings of air temperature, water temperature, humidity, and pH to be taken synchronously.

4.2.3.5 Initial Approach of the Calibration and Placement of TDS/EC Sensor

The Atlas Scientific Mini Conductivity K 1.0 Kit had to be brought in from overseas and had a wait time for its delivery, which left us with no alternative but to use a locally available, low-end TDS sensor kit.

Due to the analog nature of the low-end TDS sensor, it required calibration, and this probe is designed to have a cubic calibration graph [79]. We used 32 sample solutions of different TDS values. The solutions were prepared by adding table salt to a sample of distilled water while taking the voltage readings simultaneously using the following steps:

1. We took 250 mL of distilled water into a measuring cup and added a pinch of salt to the water, stirring it well until all of the salt appeared to dissolve.
2. A digital TDS/EC meter, previously calibrated using a standard 1382 PPM solution, was used to measure the EC of the sample solution prepared.
3. The TDS probe was fully immersed into the sample solution, and we waited 2 minutes for the voltage readings to settle. The EC reading from the digital EC meter and voltage reading from across the two electrodes of the TDS probe were recorded.
4. Another pinch of salt was added to the existing sample solution to raise its TDS value, and steps 2 and 3 were repeated until we had 32 data points that closely resembled a cubic function. All sample solutions had EC values within the range of 100 to 1,500 $\mu\text{Siemens cm}^{-1}$.

After some salt was added to the sample solution, a digital TDS/EC meter, previously calibrated using a standard 1,382 PPM solution, was used to measure the EC of the sample solution, and the corresponding voltage reading across the TDS probe was recorded. All recorded values were within the range of 100 to 1,500 $\mu\text{Siemens cm}^{-1}$.

The TDS probe was immersed into the different sample solutions. We determined the settling time for the voltage readings on the pH probe to be approximately 2 minutes. Before this time, the voltage readings are subjected to overshoots and mild fluctuations. Taking 2 minutes as the standard settling time, we took readings of the voltages produced across the two electrodes of the TDS probe from the Serial Monitor of the Arduino. The corresponding voltage readings from the 32 sample solutions are in Table 4.3.

| EC ($\mu\text{Siemens cm}^{-1}$) | Voltage (V) | EC ($\mu\text{Siemens cm}^{-1}$) | Voltage (V) |
|---------------------------------------|----------------|---------------------------------------|----------------|
| 114 | 0.38 | 818 | 1.05 |
| 122 | 0.41 | 836 | 1.07 |
| 146 | 0.46 | 866 | 1.08 |
| 162 | 0.51 | 910 | 1.09 |
| 186 | 0.57 | 936 | 1.10 |
| 266 | 0.70 | 956 | 1.11 |
| 288 | 0.72 | 996 | 1.12 |
| 364 | 0.82 | 1014 | 1.14 |
| 396 | 0.85 | 1094 | 1.17 |
| 540 | 0.92 | 1054 | 1.16 |
| 592 | 0.95 | 1126 | 1.18 |
| 644 | 0.97 | 1210 | 1.21 |
| 686 | 0.99 | 1276 | 1.22 |
| 722 | 1.00 | 1316 | 1.23 |
| 754 | 1.02 | 1360 | 1.25 |
| 772 | 1.04 | 1416 | 1.26 |

Table 4.3: Voltage readings from TDS probe calibration with 32 sample solutions with different TDS values

The 32 data points are used to make a scatterplot using Seaborn, as shown in Figure 4.24. 3rd Order Polynomial regression is applied to the scatterplot to obtain the equation relating the EC of the solution in which the TDS probe is submerged to the voltage produced across its electrodes.

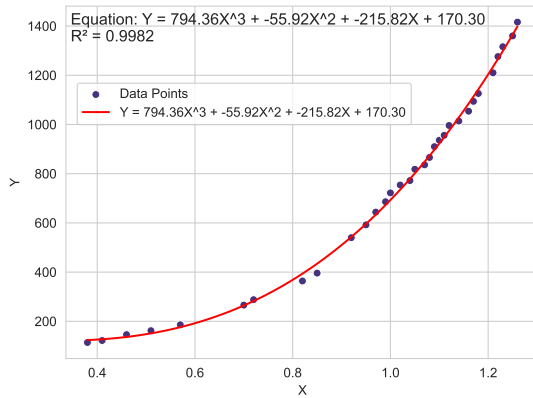


Figure 4.24: Scatterplot of EC against electrode voltage graph, plotted in Seaborn

The equation for the EC readings is determined to be:

$$y = 794.36x^3 - 55.92x^2 - 215.82x + 170.30 \quad (4.2)$$

y is the EC value of the solution, and x is the voltage produced across the electrodes of the EC probe in Volts(V). Equation 4.2 has an R-squared value of 0.9982, indicating an excellent fit for the 32 data points. Thus, this equation was used by the Arduino Nano to calculate the EC value from the voltage produced at the electrodes. The probe has an operating voltage of 3.3 to 5.5V [26].

The pH probe is held by the sensor holder, as seen in Figure 4.20, such that its tip is entirely submerged in the nutrient solution to monitor the EC of the solution. The sampling rate of the pH sensor is set at 0.05 readings every second or 1 reading every 3 minutes to allow the probe reading to settle and to allow the readings of air temperature, water temperature, humidity, pH, and EC to be taken synchronously.

4.2.3.6 Current Approach of Using the Atlas Scientific Mini Conductivity K 1.0 Kit

As we kept running our system and testing the sensors and actuators, we noticed that the readings of the low-end TDS sensor started to drift even when nothing was added to the nutrient solution. Upon investigation, we learned that this TDS probe is unsuitable for being immersed indefinitely in a solution. It is leeched off of its electrolyte and loses its calibration. It requires frequent calibration, as much as once every 5-6 hours.

As such, this sensor is unsuitable for our system, which would require the probe to be immersed indefinitely in the nutrient solution. This led us to use the Atlas Scientific Mini Conductivity K 1.0 Kit. Compared to the low-end pH sensor, the Atlas Scientific Mini Conductivity K 1.0 Kit probe could be immersed indefinitely in the nutrient solution and only required calibration once every 6 months. The Atlas Scientific Mini Conductivity K 1.0 Kit also has a more straightforward calibration process:

1. The probe is immersed into one of the 2 conductivity solutions provided at $12,880 \mu\text{Siemens cm}^{-1}$ and $80,000 \mu\text{Siemens cm}^{-1}$. The probe is connected to the signal conversion circuit board, which uses the Universal Asynchronous Receiver-Transmitter(UART) protocol to send the data to the Arduino Nano.
2. The Serial Monitor monitors the data received by the probe. The initial readings are off by a significant margin as they start to settle closer to the actual EC value of the conductivity solution.
3. Once the fluctuations in readings go down, the command “Cal,L,X” is sent to the sensor via the Serial Monitor, where L is the level of the point, which can be high, medium, or low on the calibration graph. X is the EC value of the conductivity solution. Table 4.2 below lists the 2 commands sent via the Serial Monitor for the 2-point calibration.

| EC | Calibration Command |
|--------|---------------------|
| 12,880 | Cal,low,12880 |
| 80,000 | Cal,high,80000 |

Table 4.4: List of calibration commands sent to the Atlas Scientific Mini Conductivity K 1.0 Kit

4. Upon sending the correct calibration command, the Serial Monitor responds with an “*OK” message, indicating that the single-point calibration was completed without any errors. The probe is then gently removed from the buffer solution and cleaned using distilled water.
5. The 2-point calibration is finished by repeating steps 1 through 4 for all 2 of the conductivity solutions. To check whether the overall calibration process succeeded, the EC probe is immersed into a different conductivity solution with an EC value of 1382 cm^{-1} . After a settling time of approximately 10 seconds, the sensor gave a reading of 6.85. This indicated that the calibration process was completed without any errors.

The Atlas Scientific Mini Conductivity K 1.0 sensor replaces the low-end TDS sensor. It is held by the sensor holder, as seen in Figure 4.25, so its tip is entirely submerged in the nutrient solution to monitor the EC of the solution. The sampling rate of the EC sensor is set at 0.5 readings per second or 1 reading every 2 seconds.

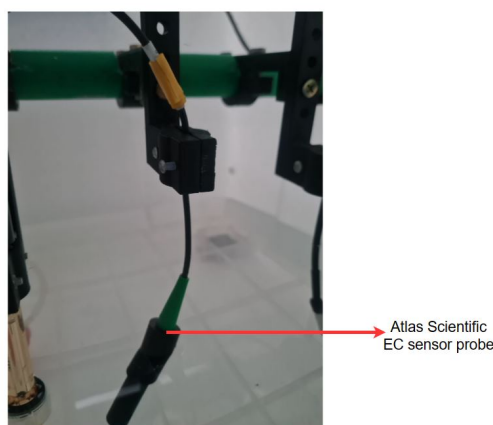


Figure 4.25: Atlas Scientific EC sensor probe fixed on the sensor holder and immersed in nutrient solution

4.2.3.7 Placement of Water Level Sensor

Our proposed system uses an HC-SR04 Ultrasonic sensor, as seen in Figure 4.26.

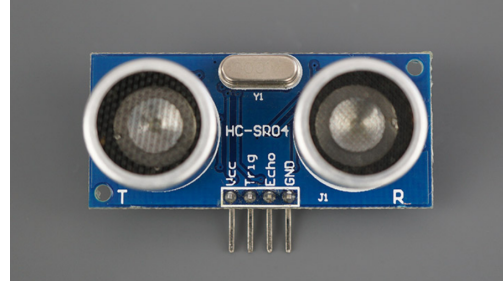


Figure 4.26: HC-SR04 Ultrasonic sensor [80]

The HC-SR04 sensor is held by the sensor holder, as seen in Figure 4.20, so it is kept at a fixed height from which it can measure the nutrient solution level left in the NSCM. The sampling rate of the ultrasonic distance sensor is set at 0.5 readings every second or 1 reading every 2 seconds.

4.2.3.8 Placement of CO₂ Sensor

Our proposed system uses an MH-Z19C NDIR CO₂ sensor, as seen in Figure 4.27. The sensor module is attached near the top corner of the sidewall of the GM. CO₂ gas tends to settle down inside crevasses and fissures. Placing the CO₂ gas sensor at that height allows us to measure the concentration of the gas dispersed throughout the GM to ensure accurate sensing of the interior environment. The sampling rate of the MH-Z19C NDIR CO₂ sensor is set at 0.5 readings every second or 1 reading every 2 seconds.



Figure 4.27: MH-Z19C NDIR CO₂ sensor mounted on the side wall of the Growth Module

4.2.3.9 Placement of the Camera

Our proposed system uses a Lenovo Select FHD Webcam [81]. It is connected to the Raspberry Pi 4 and is used to get real-time video of the interior of the GM. This video feed is embedded into the web-based dashboard from which the current state of the plants growing inside the GM can be viewed remotely. Figure 4.28 below shows the webcam being mounted near the top corner of the GM with its head tilted at an angle of depression. This allows the webcam to capture the maximum area within the GM.



Figure 4.28: Lenovo Select FHD Webcam mounted near the top corner of the Growth Module

4.2.4 Actuators

4.2.4.1 Initial Solution Cooling Approach with the Thermoelectric Peltier Water Cooler

In our proposed system, we developed a thermoelectric Peltier module-based water cooler. At the core of this cooler is the TEC1-12706 Thermoelectric Peltier cooling device. The diagram illustrates the working principle of the cooler.

Figure 4.29 shows the block diagram for the working principle of the cooler.

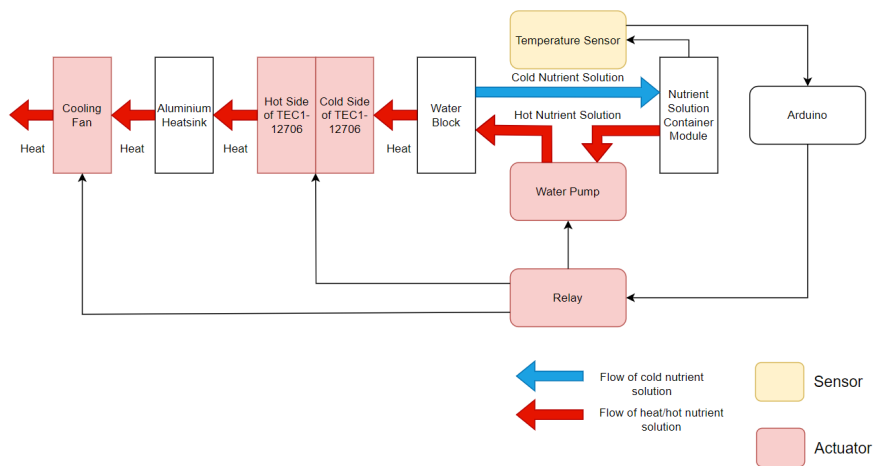


Figure 4.29: Block diagram for the thermoelectric Peltier cooler

When the temperature sensor detects a temperature rise beyond the optimal nutrient solution temperature, the Arduino sends a signal to the relay, which then turns on the submersible water pump to drive the nutrient solution from the NSCM to the water block of the cooler as well as the TEC1-12706 Peltier cooling device and cooling fan. The heat from the nutrient solution driven from the water pump is absorbed by the water block, which is in contact with the cold side of the TEC1-12706, relatively colder than the nutrient solution. This causes a cooling effect on the nutrient solution.

The hot side of the TEC1-12706 is attached to the heatsink, where heat is transferred from the hot side and is actively air-cooled using the cooling fan. As long as the heatsink is cooled, the cold side of the TEC1-12706 remains cold and keeps

cooling the nutrient solution, which is then sent back to the NSCM. This process continues until all of the nutrient solution present in both the NSCM and GM are at the same optimal temperature.

The cooler is developed as seen in Figure 4.30 and Figure 4.31. Two such coolers are developed due to the large volume of nutrient solution used in the system. Each of the coolers has an operating voltage of 12V and an operating current of 6.25A[82].

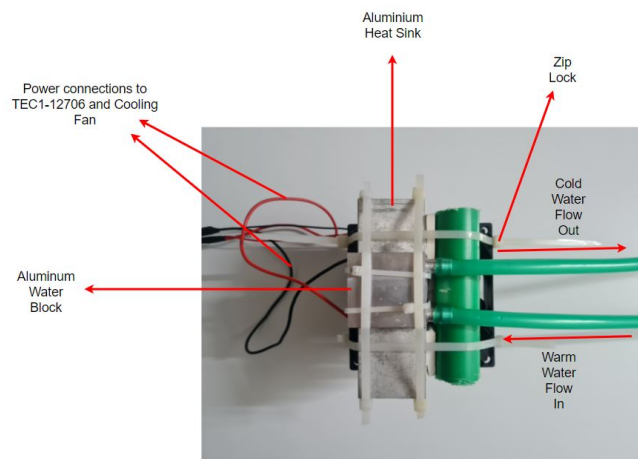


Figure 4.30: Top view of Thermoelectric Peltier Module-based Water Cooler

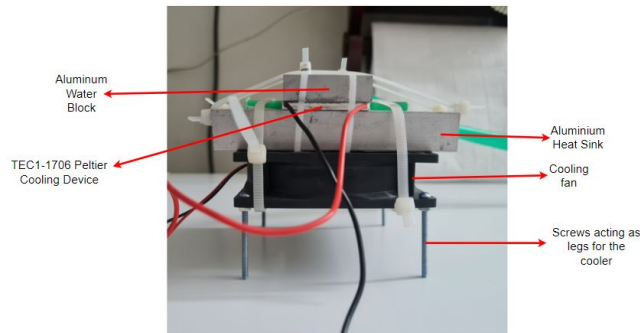


Figure 4.31: Side view of Thermoelectric Peltier Module-based Water Cooler

4.2.4.2 Current Approach of Using a Refrigerative Cooler

After running and testing the thermoelectric Peltier cooler for an extended period, we learned that the cooling capacity of the thermoelectric Peltier cooler was

insufficient to reduce the temperature of the nutrient solution to the required optimal temperature range for lettuce. This led us to procure a refrigerating aquarium cooler. We are using the Hailea HS-28A Aquarium Chiller. This chiller is designed to cool 160L of water from 28°C to 18°C in around 20 hours. For our approximately 50L of nutrient solution, this chiller was ideal for bringing the temperature down.

However, one of the challenges of keeping the temperature of the nutrient solution within the optimal range proved to be more complex than previously anticipated. As the chiller removed the heat from the nutrient solution, the heat present in the atmosphere made its way inside the NSCM, which significantly reduced the cooling capacity of the aquarium chiller. Furthermore, the heat generated by the exhaust from the chiller also adds to the heat in the surrounding atmosphere, which further reduces the overall cooling capacity of the chiller.

This problem was mitigated by introducing two design changes in the system:

1. The NSCM is placed inside a Styrofoam case. The walls of the box are approximately 45mm thick, offering adequate heat insulation to the walls of the container.
2. A high-speed desk fan was placed adjacent and perpendicular to the direction in which the chiller let out exhaust air. The fan blew the hot air away from the NSCM, preventing heat from accumulating near it.

After implementing these solutions, the chiller can now reduce the temperature of the nutrient solution from 30°C to 18°C in around 14 hours.

Figure 4.32 shows the Hailea HS-28A chiller running and drawing nutrient solution from the NSCM, which is placed inside its Styrofoam case.

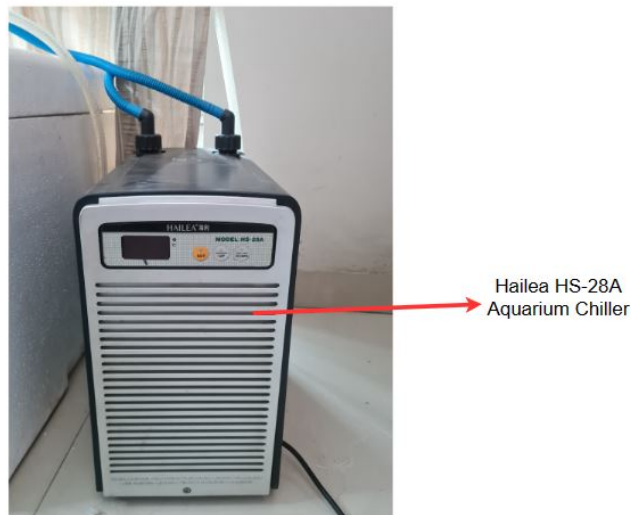


Figure 4.32: Hailea HS-28A Aquarium Chiller placed beside the NSCM

4.2.4.3 Thermoelectric Peltier Air Cooler

We developed a thermoelectric Peltier module-based air cooler. At the core of this cooler is the TEC1-12715 Thermoelectric Peltier cooling device and two DeepCool AK400 Performance CPU coolers.

Figure 4.33 shows the block diagram for the thermoelectric Peltier module-based air cooler.

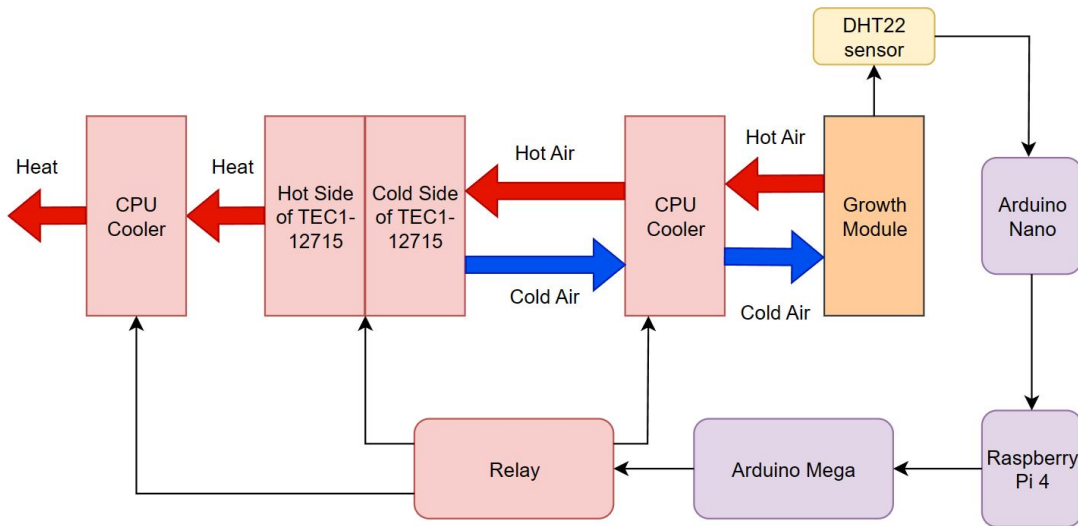


Figure 4.33: Block Diagram for the thermoelectric Peltier Air Cooler

When the DHT22 sensor detects a temperature rise beyond the optimal air temperature inside the GM, the Arduino Nano sends a signal to the Raspberry Pi. The Pi, in turn, sends the actuation signal to the Arduino Mega, which actuates the relay. The relay then powers the two CPU coolers and TEC1-12715 module. The cooler inside the GM pulls in the hot air and forces it to come in contact with the relatively cold side of the TEC1-12715. This causes heat exchange between the air inside and the TEC1-12715.

Another CPU cooler is constantly cooling the hot side of the TEC1-12715. As long as the hot side of the TEC1-12715 is cooled, the cold side of the TEC1-12715 remains cold and keeps cooling the air inside the GM. This process continues until all of the air inside the GM is at the same optimal temperature.

Figure 4.34 shows the Air Cooler attached to the top corner of the GM. That particular spot was chosen to ensure that the hot air rising at the top cooled while ensuring the LED arrays were not obstructed. A connector board was designed and developed, as seen in Figure 4.35 below, which allows the native connector of the CPU coolers themselves to be connected directly to the power source via the relay. This allows for more accessible connections in the system, which can be easily undone to allow for greater mobility when moving the system.

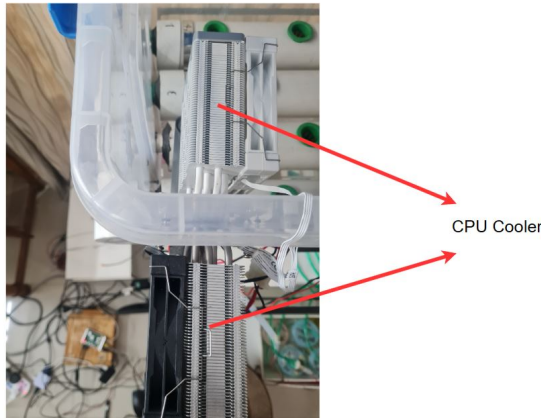


Figure 4.34: Air Cooler attached to the side of the GM

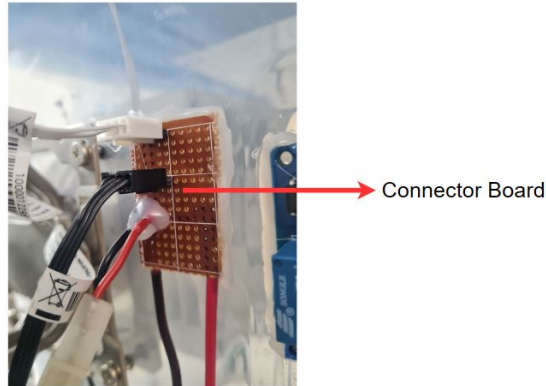


Figure 4.35: Air Cooler attached to the side of the GM

The air cooler we built also acts as a dehumidifier. During its testing, we observed that it produced condensation inside the GM, reducing the amount of water vapour present inside. Thus, we are also using the air cooler as our dehumidifier instead of introducing a dedicated humidifier.

The TEC1-12715 Peltier modules have a maximum current rating of 15A [83]. We used a 12V 30A Industrial Switch-Mode Power Supply (SMPS) to provide this module with sufficient current, as seen in Figure 4.36.



Figure 4.36: SMPS 30A Power Supply

4.2.4.4 Initial Approach for the Nutrient and Acid/Base Dosing System

In our proposed system, we developed a dosing system that adds a concentrated nutrient solution, acid or base to the nutrient solution in the NSCM. A 5V micro-submersible DC Water Pump is at the core of the dosing system.

The dosing system comprises 5 reservoirs for 5 different concentrated solutions:

1. Nutrient solution A
2. Nutrient solution B
3. 0.1 Mol L^{-1} solution of Nitric acid(HNO_3) of pH 1.0
4. 10 Mol L^{-1} solution of Sodium Hydroxide(NaOH) of pH 13.0
5. Distilled water of pH 7.0

The components used in the dosing system are:

1. 5 x 2L Polypropylene container with lids
2. 5 x 5V Micro Submersible DC Water Pump
3. 2 x 5V 4-channel relay module

4. 8mm tubing

Figure 4.37 shows a block diagram illustrating the working mechanism of the dosing system.

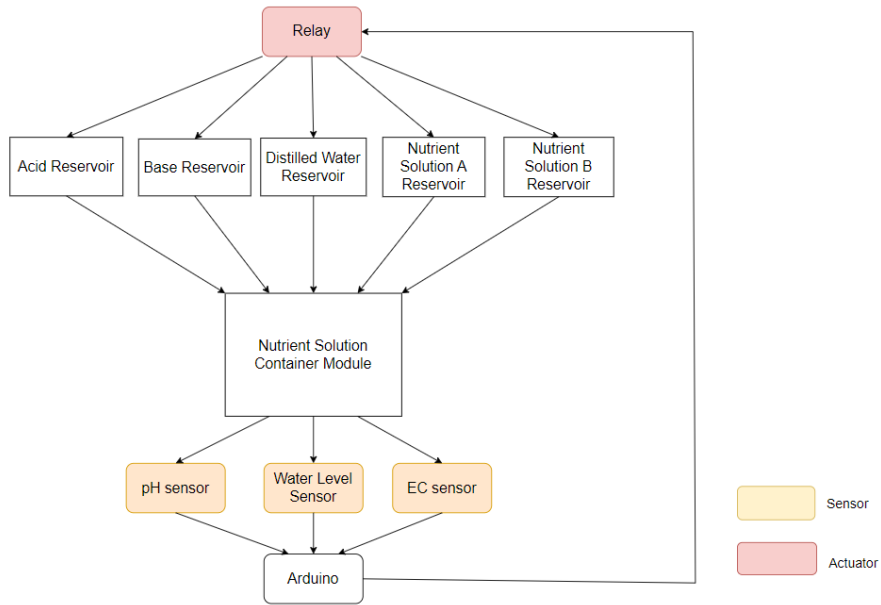


Figure 4.37: Block diagram of the dosing system

A submersible water pump is fully submerged in the solution for each reservoir, as seen in Figure 4.37. The pH, water level and EC sensors monitor the status of the nutrient solution present in the NSCM. Whenever the pH, EC or water level changes beyond the set thresholds, the Arduino sends a signal to the relay module, which turns on the submersible water pump of the required solution reservoir.

The duration the relay turns on the water pump is predetermined to allow for small doses of each solution into the NSCM. If needed, the relay will enable pulses of current to the water pumps to provide as many doses of solution as required by the nutrient solution to reach optimal conditions.

The submersible water pumps are connected in parallel. The operating voltage of the doser system is 5V, and the operating current is 1A [84] in the case where all five submersible pumps are turned on. The doser system is developed and kept beside the NSCM at the same horizontal, as shown in Figure 4.38.

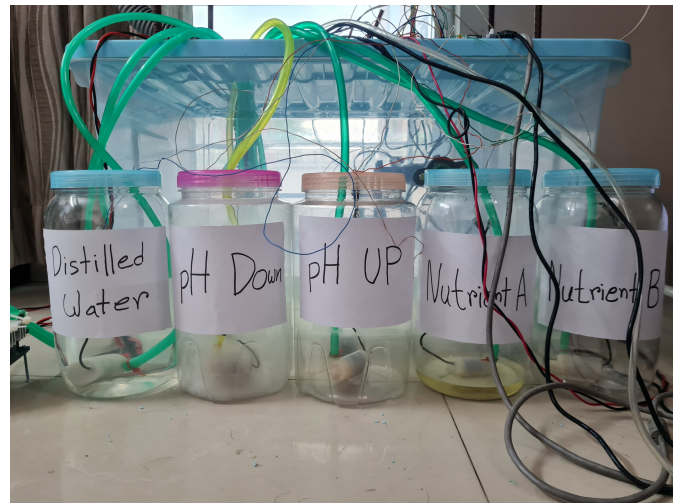


Figure 4.38: Nutrient and Acid/Base Dosing System

4.2.4.5 Current Approach for the Nutrient and Acid/Base Dosing System

The 5V micro-submersible pumps were mounted to the bottom of the Polypropylene containers using an adhesive. After running the system for an extended period, we discovered that the 5V micro-submersible pumps would slip out from the bottom. This would cause the pumps to rise back up due to being lightweight, and they would not be able to pump the required solutions when needed. Furthermore, the tubing would also slip out of the pumps, rendering the pumps useless.

This problem was mitigated by using 5V vacuum air pumps instead. These pumps were attached to the lids of the containers and can efficiently pump the required solution from the containers to the NSCM when needed. Additionally, the Dosing System was placed inside a box to provide better accessibility and portability, as now all 5 containers can be moved together if needed.

Figure 4.39 and 4.40 show the new design of the dosing system with the 5V vacuum pumps on top of the lids from the top and side view. The current design allows the dosing system to be placed in a more space-efficient manner next to the NSCM.



Figure 4.39: Top view of the new Dosing System



Figure 4.40: Side view of the new Dosing System

4.2.4.6 Automated Multi-plug for High Power Components

Some of the components used in the system come with non-detachable power plugs. Removing these power plugs to power and actuate them, per requirement, using their wires appeared redundant to us since the power plugs were of reasonable quality, and some even had fuses to protect the components from electrical surges.

Therefore, we developed an automated multi-plug using a regular multi-plug and controlling its individual power sockets using a 12V 4-channel relay. The switches

of the individual power sockets are replaced with the relays. So when signals to actuate the components connected to this multi-plug are sent to the relay, the circuit for that power socket is complete, providing power to that component.

Figure 4.41 shows the automated multi-plug, powering the aquarium chiller, high-speed fan, and LED grow lights.

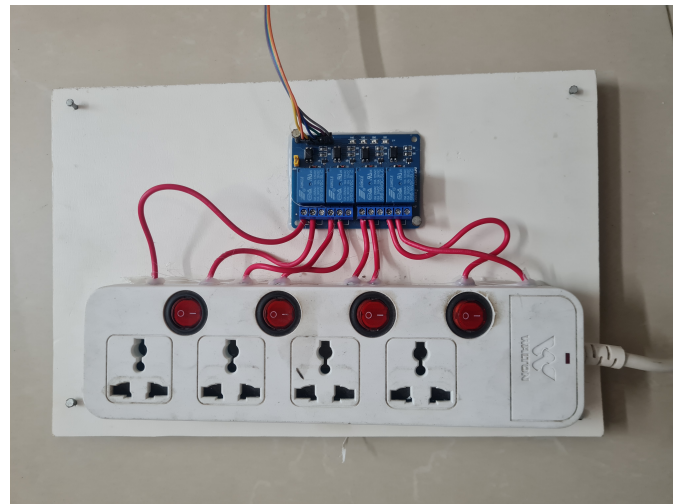


Figure 4.41: Automated Multiplug

4.2.4.7 Grow Lights

The system is equipped with 2 Auoyo 40W LED Growlight lamps. These lamps are bolted on the lid of the GM and placed so that the light spreads out and is incident on all of the plants equally.

Figure 4.42 shows the Grow lights mounted on the lid of the GM.

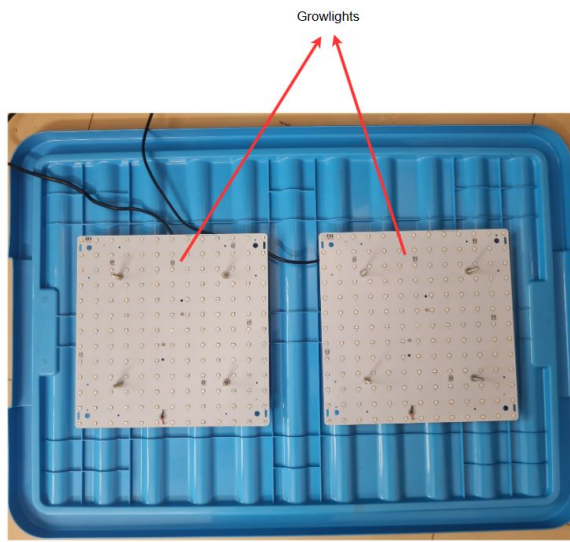


Figure 4.42: Grow Lights mounted under the lid of the Growth Module

The grow lights are powered using the automated multi-plug, with the relay controlling the ON/OFF cycle of the lights. For lettuce, the optimal light cycle is 16 hours of light, referred to as the photoperiod, followed by 8 hours of darkness [85].

4.2.4.8 CO₂ Gas Delivery System

The system has a 4 kg cylinder of CO₂ gas. The cylinder is equipped with a 12V pressure regulator with a solenoid valve. The said valve, normally closed, opens when power is supplied. The actuation of this solenoid valve is controlled via the Arduino microcontroller through the Raspberry Pi, which is fed data from the CO₂.

Figure ?? below shows the CO₂ gas delivery system. A tubing connects the CO₂ gas cylinder to the GM. When the CO₂ concentration falls below the optimal range, the solenoid valve is powered, which opens the valve. The CO₂ gas is then delivered into the GM via the tubing, which leads to an uptick in the readings from the CO₂ sensor. The solenoid valve is powered off when the readings are within the optimal range or even when they occasionally exceed it. For our system, we set the optimal range for the CO₂ concentration between 1900 PPM and 2000 PPM.

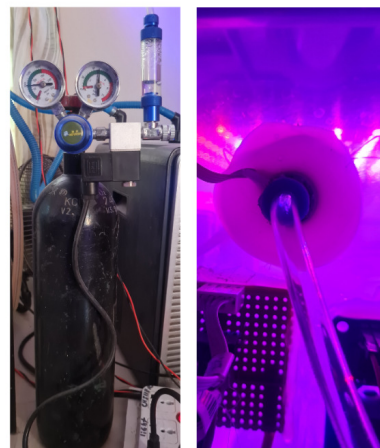


Figure 4.43: CO₂ delivery system. The CO₂ cylinder (left) is connected via tubing to the GM (right)

4.2.5 Electrical System Schematic

4.2.5.1 Sensor Board Design

The schematic for the sensor board is designed to house the humidity, water temperature, water level, pH and EC sensors. The schematic can be seen in Figure 4.44.

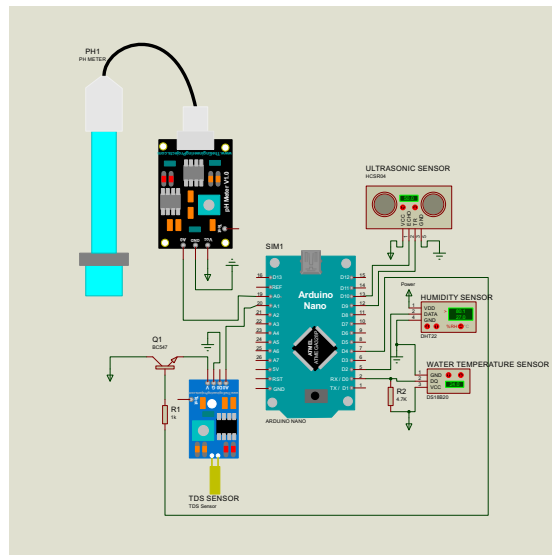


Figure 4.44: Schematic for the sensor board, designed in Proteus 8 Professional

As mentioned in the section where the working principle of the TDS sensor was explained, the probe introduces a small electric charge into the solution being measured. While testing our system, we noticed that this greatly disrupts the readings of the analog pH probe, which often gives readings of pH values highly exceeding the range of 0-14. Even allowing the V_{cc} pin of the TDS probe to have the smallest current led to this problem as the probe kept producing the electric charge into the nutrient solution. This led us to develop a solution to overcome this problem: using a Bi-Polar Junction Transistor(BJT) transistor to switch the TDS sensor.

As seen in Figure 4.44, a BC547 BJT has its Emitter pin connected to the V_{cc} pin of the TDS sensor. When the pH meter takes its readings, the NPN transistor is kept in its “OFF” state by applying zero voltage to its Base pin. After the pH reading is taken, the Arduino Nano sends a digital signal from its D4 pin to the Base pin to flip the BJT to its “ON” state and allow current to flow into the V_{cc} pin of the TDS sensor, allowing it to take readings from the nutrient solution.

Since the previous low-end pH and TDS sensors were replaced with the Atlas Scientific pH and Conductivity sensor kits, we no longer require the BJT gate to control the sensing actions.

As seen in Figures 4.45 and 4.46, the sensor board was developed on a single-side circuit board by soldering Printed Circuit Board(PCB) connectors to the circuit board and then attaching jumper wires and the Arduino Nano to them.

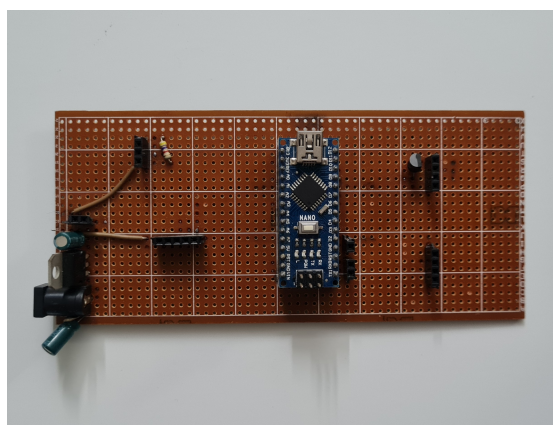


Figure 4.45: Top view of the sensor board

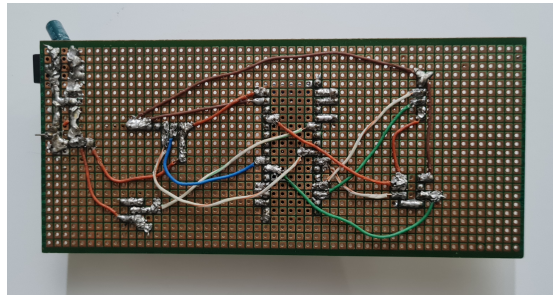


Figure 4.46: Bottom view of the sensor board

4.2.5.2 Actuator Board Design

Like the sensor board, an actuator board was also designed and developed to house the Arduino Mega microcontroller, to which all the actuators used in our system are connected. Figure 4.47 below shows the actuator board housing the Arduino Mega and the JST connectors. The latter makes it easy to attach and detect the connector pins extended from the actuators, making assembly and disassembly less time-consuming. This also makes the system expandable since more JST connectors can easily be soldered onto the board to house more actuators.

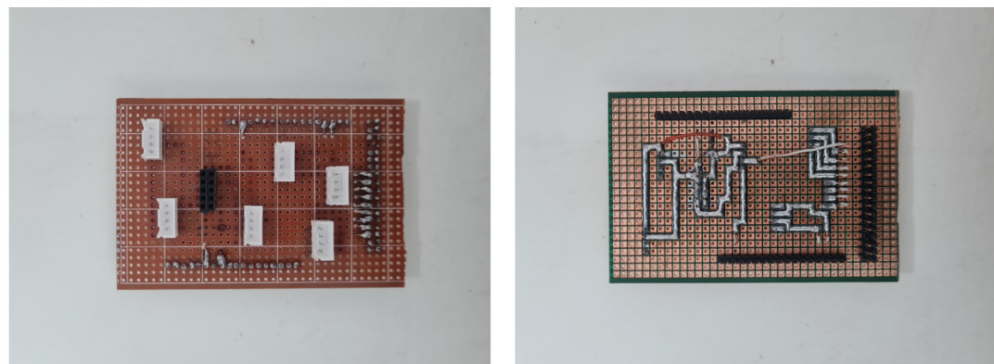


Figure 4.47: The top view of the actuator board (left) and the bottom view of the actuator board (right), which shows the soldered connections between the pins of the Arduino Mega and the JST connector pins

4.2.6 Microcontrollers

4.2.6.1 Using a Raspberry Pi 4 as the Central Control Unit

A Raspberry Pi 4B 4GB model is used as the Central Control Unit for the system. The Arduino Nano receives data from the sensors, which it feeds to the Raspberry Pi. The Raspberry Pi then decides on the control action to be taken and sends the actuation signals to the Arduino Mega, which controls the actuators. The connections between the Raspberry Pi, Arduino Nano and Mega use USB cables. This is because the USB protocol ensures that the data transfer between the various controllers does not allow any garbage values due to the checksums being performed during data transmission.

Figure 4.48 shows that the Raspberry Pi is connected to the Arduino Nano and Arduino Mega.

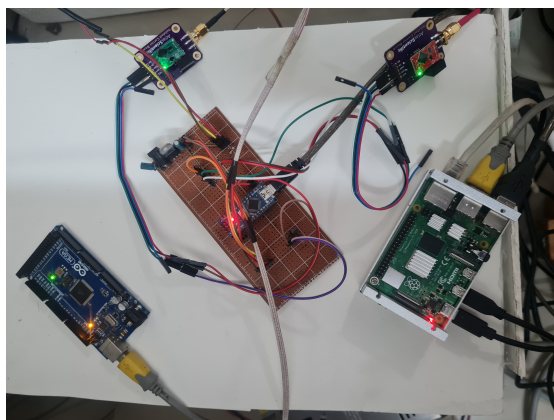


Figure 4.48: Raspberry Pi connected with the Arduino Nano and Arduino Mega

4.2.6.2 Using a Raspberry Pi as an Internet of Things (IoT) Gateway

The sensor data collected by the Raspberry Pi from the Arduino Nano are sent to a ThingSpeak channel. Thingspeak is an IoT analytics platform that takes sensor data into fields, offering visualization tools and widgets. These visualizations and widgets can be used to generate custom dashboards and websites to monitor sensor data. The visualizations and widgets generated from data sent by the Raspberry Pi are then embedded into a custom web-based dashboard that we developed. The

sensor data sent to the Thingspeak channel is saved on-site and can be exported as a Comma-Separated Value (CSV) file.

Figure 4.49 shows the block diagram illustrating the data flow between the Raspberry Pi, Arduino microcontrollers and ThingSpeak.

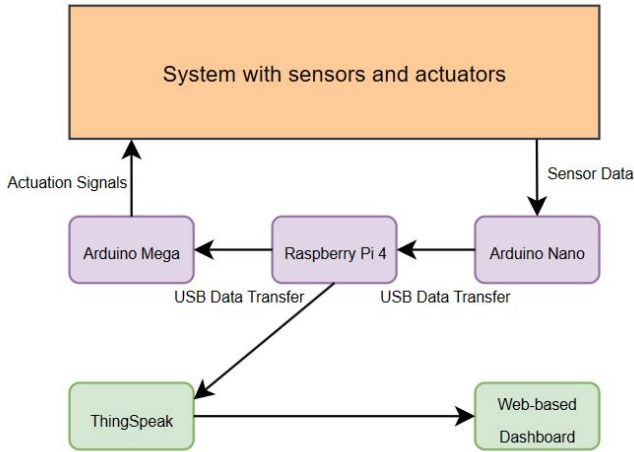


Figure 4.49: Block diagram illustrating the flow of data between the Raspberry Pi, Arduino microcontrollers and ThingSpeak

We developed a web application using Flask, a microweb framework written in Python. This application is the backend of the web-based dashboard that we developed for our system. This web application streams the video feed from the webcam to the dashboard where it is embedded, as can be seen in Figure ???. The dashboard also processes requests from the end of the dashboard to the web application, as it allows the user to choose scripts to run. Each script is tailored with the optimal growth parameter values for different plants, allowing a wide array of plants to be grown inside the system.

Figures 4.50 and 4.51 show the dashboard with the visualizations and widgets from ThingSpeak. The data sent by the Arduino Nano to the Raspberry Pi are dummy values, so the graphs look irregular. The values were sent to test the responsivity of the website as well as that of ThingSpeak. Using the free license of ThingSpeak allows the Raspberry Pi to send data to the channel once every 15 seconds.

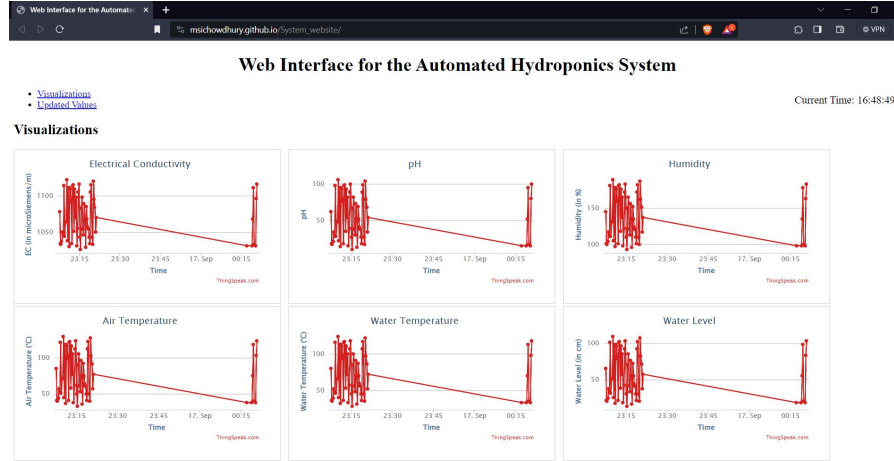


Figure 4.50: Web-based dashboard showing the visualizations from ThingSpeak from sensor data

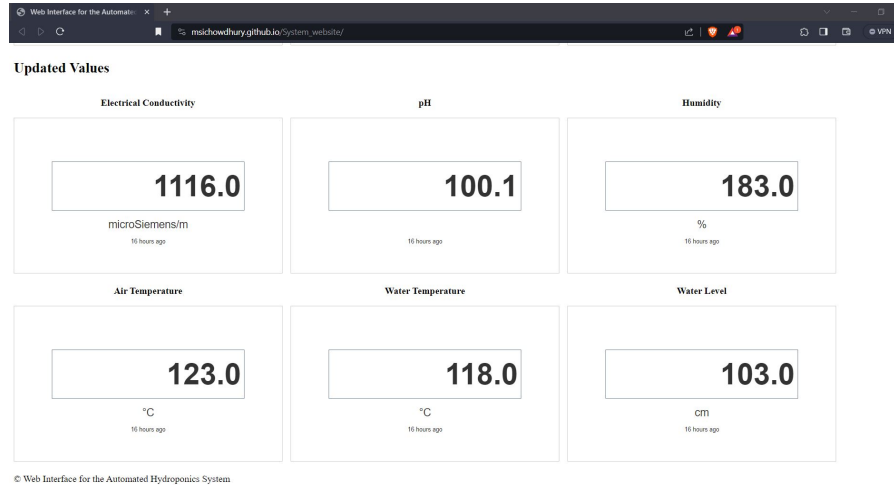


Figure 4.51: Web-based dashboard showing the widgets from ThingSpeak from sensor data

4.2.7 Current Setup of the System

A metal frame was built to accommodate the NSCM and GM vertically, keeping the GM on top. Figure 4.52 shows the metal frame holding the two modules. The frame design allows for the NSCM to be slid right between its legs, while the thickness of the rods used to make the frame easily supports the weight of the GM.

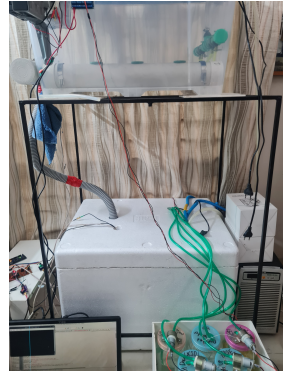


Figure 4.52: Front view of the metal frame housing the NSCM and supporting the GM

Figure 4.53 shows the current setup of the system. The GM is placed on top of the metal frame. The connections between the sensors, actuators, Arduino Nano, Mega and Raspberry Pi are made before we power up the system.



Figure 4.53: Front view of the current setup of the system

4.2.7.1 Trial Run of the System

The system was powered on to test whether all the components were correctly connected. The Raspberry Pi is booted on as it receives the signals from the sensors via the Arduino Nano. The web-based dashboard then started to update the values in the visualization graphs and widget, indicating that the Raspberry Pi was reading the data and sending the readings to the ThingSpeak channel. The results from the sensor readings are discussed in detail in the next chapter.

4.3 Experimental Design

In order to thoroughly evaluate the performance of our implemented system, we designed an experiment: 42 Green Leaf lettuce seedlings were randomly divided into 3 equal batches of 14 seedlings. Each of these batches was then transplanted into the following three treatments on the same day:

1. P1: Our automated system
2. P2: 25% Soil + 75% cow manure compost in pots
3. P3: Manual Deep Water Culture (DWC) hydroponics system

Lettuce plants in P2 and P3 were kept at the same location to ensure equal exposure to sunlight, temperature, humidity, and ambient CO₂ concentration. The nutrient solution used in P1 and P2 was prepared using the concentrated solution of Nutrient A and B, ensuring that the initial EC value of both solutions is kept as close as possible. Data collection was done on a daily basis, from the day after the Day of Transplant (DAT). The growth of all the plants in each of these batches was monitored using:

1. Leaf Area: The area covered by the lettuce leaves was determined from overhead images of the batches. FIJI (FIJI Is Just ImageJ) [86], an open-source image processing package, was used to measure the leaf area from the pixel area calculated from the images, which is converted into squared centimeters (cm²) from scaling. Figure 4.54 shows the package in action in determining the leaf area of one of the lettuce plants.

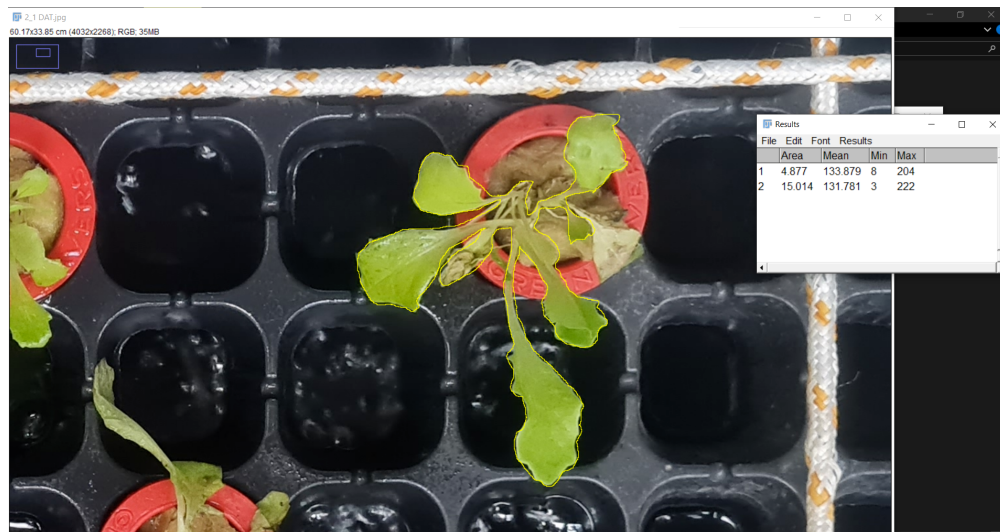


Figure 4.54: Leaf area of a plant being measured using FIJI

2. Number of leaves: Only the leaves that appear healthy and are 2 cm or greater in length are counted.
3. Fresh weight: This is the total weight of the biological material of the plant when it is harvested from the medium. The leaves, stems, roots and any other parts of the plant are weighed before any of the water content within the plant is lost to obtain this value. This was determined by taking 3 random replicates from each of the 3 batches, getting their mass using an electronic mass balance, and calculating the mean fresh weight of the plants belonging to each batch. This is measured in grams (g).
4. Dry weight: This is the weight of the plant after all the water content has been removed from its tissues. This value provides a better representation of the biomass of the plant and its nutritional content. This was determined by taking 3 random replicates from each of the 3 batches, placing them in an oven at a temperature of 70°C for 48 hours, then weighing them using an electronic mass balance. This is measured in grams (g).
5. Dry matter: This is the weight of all the solid, non-water components in the plant tissues. It represents the total biomass of the plant without the water content.

$$\text{Dry Matter \%} = \left(\frac{\text{Dry Weight}}{\text{Fresh Weight}} \right) \times 100$$

Due to the destructive nature of the measurement techniques for fresh weight, dry weight, and dry mass, these readings were taken after the harvest. Leaf area and number of leaves were recorded daily. After the harvest, a comparison was also done for the true leaf area, as the measurements made daily were subject to errors due to the curling of the leaves or their overlapping over one another, which was indiscernible from the overhead images.

Chapter 5

Results

In this chapter, we will break down the results that we have obtained from the ongoing implementation of the system. The results below are from the time the system underwent a trial run.

5.1 Real-time Monitoring of the Physical Parameters

The sensor readings were being sent to ThingSpeak by the Raspberry Pi. ThingSpeak then creates six different real-time visualizations of the sensor data and six different widgets, each pair of visualization and widget displaying the trend and current value sent by a sensor. Figures 5.1 and 5.2 below show the web-based dashboard displaying the sensor readings right after the system is turned on. There is a 15-second delay between the updates on the website, as the free license of ThingSpeak can only fetch data once every 15 seconds.

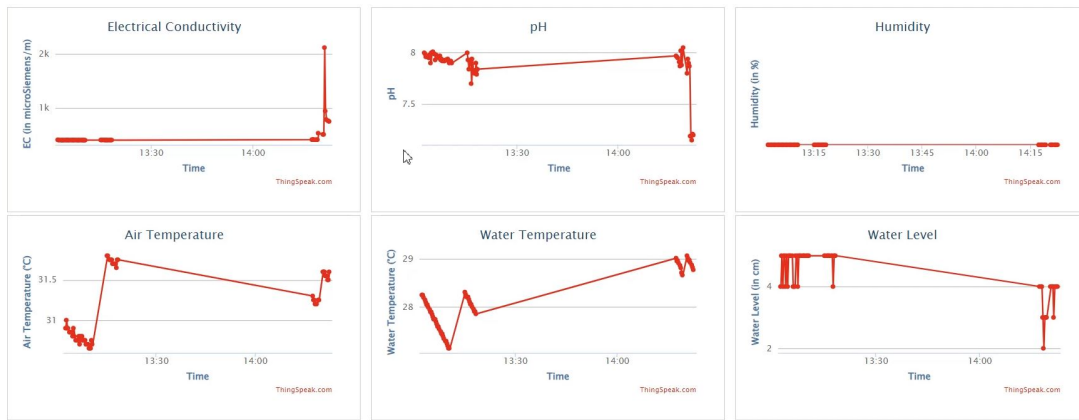
Visualizations

Figure 5.1: Graphs on the web-based dashboard show the initial values taken by the sensors

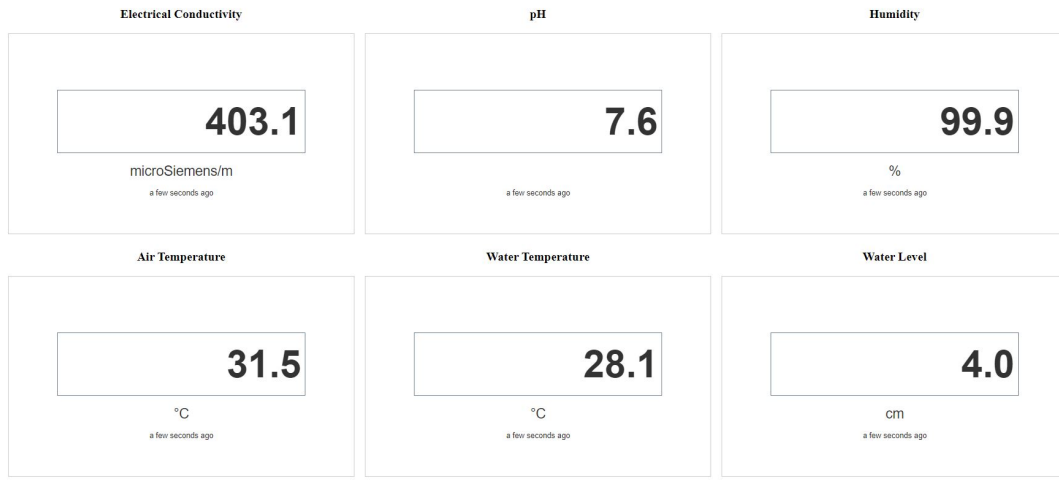
Updated Values

Figure 5.2: Widgets on the web-based dashboard show the initial values taken by the sensors

As the physical parameters are not in the optimal range at the initial stage of starting the system, the Raspberry Pi sends signals to the actuators to change these physical parameters and bring them to the optimal range. The change in the sensor readings can be observed after a while, as the graphs on the website show that the physical parameters are gradually changing and coming closer to the optimal range.

Figures 5.3 and 5.4 show the website with graphs indicating a change in physical conditions within the system after running the system for approximately 1 hour.

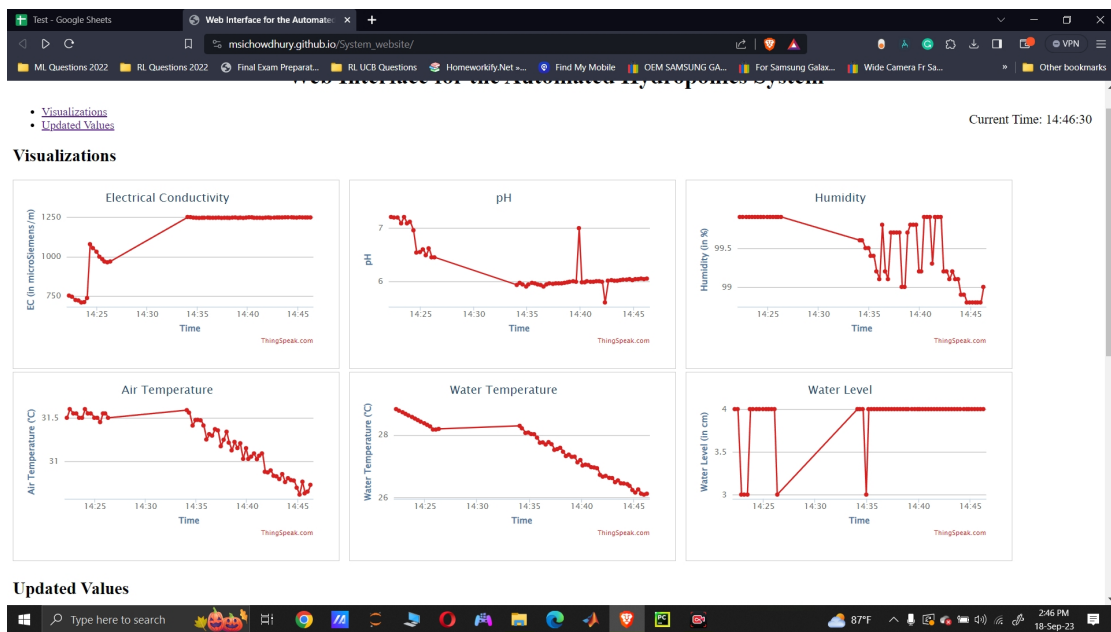


Figure 5.3: Graphs on the web-based dashboard show the values settling down taken by the sensors

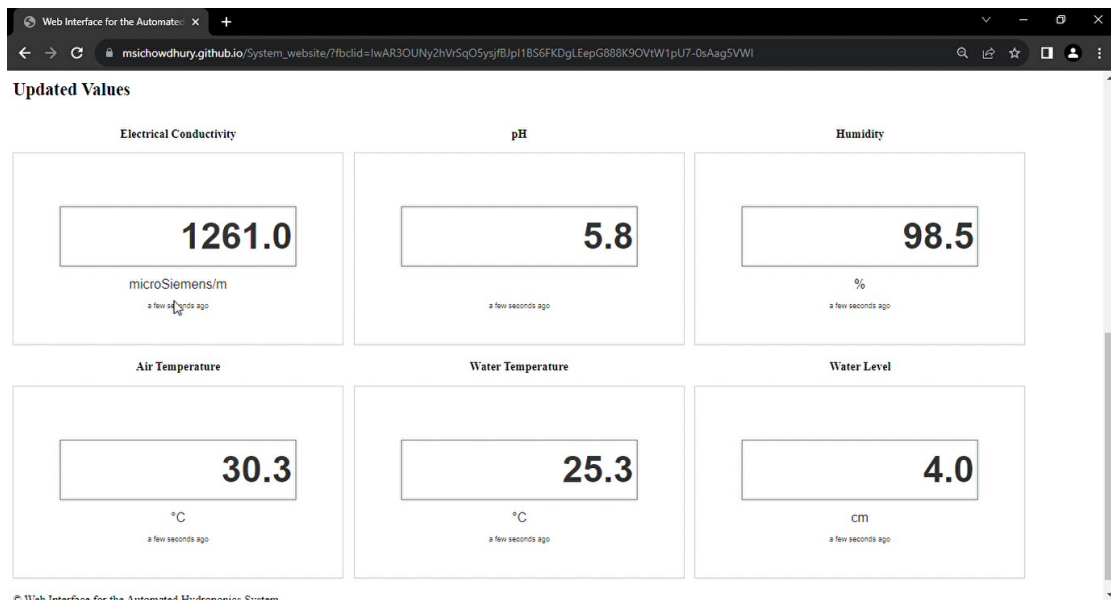


Figure 5.4: Graphs on the web-based dashboard show the values settling down taken by the sensors

5.2 Collection of Sensor Data in Google Sheets for Current Database and Future Dataset

The sensor data is sent and appended to a Google Sheet once every 2 seconds. The Google Sheet acts as a database to store all the sensor data. The control actions determined by the Raspberry Pi are also appended to each row of the Google Sheet with its corresponding sensor data.

This Google Sheet will later be exported and used as a tabular dataset to train an intelligent classification algorithm which will predict the control action to be taken by the Raspberry Pi without requiring explicit if-else conditional programming. Figure 5.5 shows the Google Sheet, updated in real-time by the Raspberry Pi.

| | A | B | C | D | E | F | G | H | I |
|-----|-----------|-------|------|----------|-----------------|-------------------|-------------|---|---|
| 1 | Timestamp | EC | pH | Humidity | Air_Temperature | Water_Temperature | Water_Level | | |
| 142 | 08:04:19 | 378.6 | 7.28 | 99.9 | 27.85 | 26.72 | 5 | | |
| 143 | 08:04:21 | 376.6 | 7.28 | 99.9 | 27.85 | 26.72 | 5 | | |
| 144 | 08:04:23 | 376 | 7.34 | 99.9 | 27.85 | 26.72 | 5 | | |
| 145 | 08:04:25 | 378 | 7.28 | 99.9 | 27.85 | 26.72 | 5 | | |
| 146 | 08:04:27 | 377.8 | 7.34 | 99.9 | 27.85 | 26.72 | 5 | | |
| 147 | 08:04:29 | 375.8 | 7.28 | 99.9 | 27.85 | 26.72 | 5 | | |
| 148 | 08:04:31 | 377.1 | 7.28 | 99.9 | 27.85 | 26.72 | 5 | | |
| 149 | 08:04:33 | 375.6 | 7.37 | 99.9 | 27.85 | 26.72 | 5 | | |
| 150 | 08:04:35 | 375.1 | 7.32 | 99.9 | 27.85 | 26.72 | 5 | | |
| 151 | 08:04:37 | 376.2 | 7.28 | 99.9 | 27.85 | 26.72 | 5 | | |
| 152 | 08:04:39 | 375.1 | 7.28 | 99.9 | 27.8 | 26.67 | 5 | | |
| 153 | 08:04:41 | 376.5 | 7.34 | 99.9 | 27.8 | 26.67 | 5 | | |
| 154 | 08:04:43 | 378.9 | 7.31 | 99.9 | 27.8 | 26.67 | 5 | | |
| 155 | 08:04:45 | 377.1 | 7.32 | 99.9 | 27.8 | 26.67 | 5 | | |
| 156 | 08:04:47 | 378.1 | 7.32 | 99.9 | 27.8 | 26.67 | 5 | | |
| 157 | 08:04:49 | 377.5 | 7.29 | 99.9 | 27.8 | 26.67 | 5 | | |

Figure 5.5: Google Sheet showing the sensor data being stored along with timestamps

Chapter 6

Conclusion

Our proposed system can lead to a new paradigm in agriculture, specifically in regions with a growing need for food with a declining or already scarce availability of arable land. Moreover, it will be highly water-efficient due to the closed nature of the system, making it highly resistant to pest infestations. Plant growth cycles will also be much shorter than traditional land-based farming and even noticeably shorter than conventional, non-automatic, and automatic hydroponic systems. In our future work, we intend to automate our system while implementing the IoT framework to make the system accessible remotely. At its final stage, we plan to implement a system where multiple GMs can grow distinct species of plants at their unique optimal conditions.

Until now, we have been able to monitor and regulate pH, nutrient solution temperature, air temperature, EC, humidity and light cycle. With this, we have completed the automation segment of the Nutrient Solution Container Module and nearly completed the automation segment of the Growth Module. We also developed a web-based dashboard to monitor the physical conditions inside the system. Given its current extent of automation, we intend to test our system to make it more robust so that greater levels of automation can be easily integrated into it.

As we advance, we plan on increasing the IoT capabilities of the system. We intend to use a camera to send a live feed to the web-based dashboard we developed. The camera feed will allow us to manually monitor the growth and status of the

plants. If time allows, we will implement a computer vision approach to monitor the growth rate of the plants automatically.

By planting a batch of plants in soil using natural fertilizers, we will compare the growth rates of both these plants and express it graphically to show how well our proposed system will work compared with traditional farming. The sensor data collected from our system will be used to make a dataset on which we will train a Machine Learning model, which would later independently determine the control actions needed by the Raspberry Pi without the need for explicit conditional programming.

Upon sufficient scaling, our proposed system will be able to produce a large quantity of produce within a markedly shorter duration than conventional methods. This would contribute towards greater food security and ensure that produce is always of the best possible quality without adding pesticides. A scaled-up version of the system can also act as a local food source for a block or perhaps a neighbourhood and ensure local food security and sovereignty.

Bibliography

- [1] C. Boylan, “The Future of Farming: Hydroponics,” Princeton Student Climate Initiative. <https://psci.princeton.edu/tips/2020/11/9/the-future-of-farming-hydroponics>, [Online] Accessed: 7-April-2023.
- [2] A. Shrestha, “Hydroponics,” Oklahoma State University Extension. <https://extension.okstate.edu/fact-sheets/hydroponics.html>, [Online] Accessed: 9-April-2023.
- [3] “Small-scale hydroponics,” University of Minnesota Extension. <https://extension.umn.edu/how/small-scale-hydroponics>, [Online] Accessed: 9-April-2023.
- [4] W. Lommen, “The canon of potato science: 27. hydroponics,” Potato Research 50 (2007) 3/4, vol. 50, no. 10, 2007.
- [5] R.-D. Alfredo, “Chapter 20 - peruvian hydroponics: low-cost options to produce vegetables for south american cities,” in Urban and Regional Agriculture. Academic Press, 2023, pp. 561–594.
- [6] G. Niu and J. Masabni, “Chapter 9 - hydroponics,” in Plant Factory Basics, Applications and Advances. Academic Press, 2022, pp. 153–166.
- [7] eff Birkby, “VERTICAL FARMING,” National Sustainable Agriculture Information Service. <https://attra.ncat.org/publication/vertical-farming/>, [Online] Accessed: 10-April-2023.
- [8] “Environmental factors affecting plant growth,” Oregon State University Extension. <https://extension.oregonstate.edu/gardening/techniques/environmental-factors-affecting-plant-growth>, [Online] Accessed: 10-April-2023.

- [9] E. B. Barbier, “Explaining agricultural land expansion and deforestation in developing countries,” *American Journal of Agricultural Economics*, vol. 86, no. 5, pp. 1347–1353, 2004.
- [10] C. Boylan, “A LOOMING FOOD CRISIS,” International Monetary Fund (IMF). <https://www.imf.org/en/Publications/fandd/issues/2022/09/Cafe-Econ-a-looming-Food-Crisis>, [Online] Accessed: 10-April-2023.
- [11] J. Campbell, J. Berry, U. Seibt, S. J. Smith, S. Montzka, T. Launois, S. Belviso, L. Bopp, and M. Laine, “Large historical growth in global terrestrial gross primary production,” *Nature*, vol. 544, no. 7648, pp. 84–87, 2017.
- [12] V. Palande, A. Zaheer, and K. George, “Fully automated hydroponic system for indoor plant growth,” *Procedia Computer Science*, vol. 129, pp. 482–488, 2018.
- [13] D. J. G. Janice Easton, “PLANT CONNECTIONS LEADER’S GUIDE—LESSON 3: WHAT MAKES PLANTS GROW?” University of Florida Institute of Food and Agricultural Sciences Extension. <https://edis.ifas.ufl.edu/publication/4H360>, [Online] Accessed: 10-April-2023.
- [14] P. J. White and P. Brown, “Plant nutrition for sustainable development and global health,” *Annals of botany*, vol. 105, no. 7, pp. 1073–1080, 2010.
- [15] R. Sutulienė, K. Laužikė, T. Pukas, and G. Samuolienė, “Effect of light intensity on the growth and antioxidant activity of sweet basil and lettuce,” *Plants*, vol. 11, no. 13, p. 1709, 2022.
- [16] A. Nafiu, O. Togun, M. Abiodun, V. Chude et al., “Effects of npk fertilizer on growth, drymatter production and yield of eggplant in southwestern nigeria.” *Agriculture and Biology Journal of North America*, vol. 2, no. 7, pp. 1117–1125, 2011.
- [17] A. Isah, E. Amans, E. Odion, and A. Yusuf, “Growth rate and yield of two tomato varieties (*lycopersicon esculentum* mill) under green manure and

- npk fertilizer rate samaru northern guinea savanna,” International Journal of Agronomy, vol. 2014, 2014.
- [18] E. C. Cocking, “Helping plants get more nitrogen from the air,” European Review, vol. 8, no. 2, p. 193–200, 2000.
- [19] M. T. John Sawyer, John Creswell, “Phosphorus Basics,” Iowa State University Extension and Outreach.<https://crops.extension.iastate.edu/encyclopedia/phosphorus-basics>, [Online] Accessed: 18-June-2023.
- [20] S. A. Barber, The Role of Potassium in Agriculture. USA: Wiley, January 1968.
- [21] V. Tabaglio, R. Boselli, A. Fiorini, C. Ganimede, P. Beccari, S. Santelli, and G. Nervo, “Reducing nitrate accumulation and fertilizer use in lettuce with modified intermittent nutrient film technique (nft) system,” Agronomy, vol. 10, no. 8, p. 1208, 2020.
- [22] B. D. Hardeep Singh, “Electrical Conductivity and pH Guide for Hydroponics,” Oklahoma State University Extension. <https://extension.okstate.edu/fact-sheets/electrical-conductivity-and-ph-guide-for-hydroponics.html>, [Online] Accessed: 18-June-2023.
- [23] A. Marandi, M. Polikarpus, and A. Jõeleht, “A new approach for describing the relationship between electrical conductivity and major anion concentration in natural waters,” Applied geochemistry, vol. 38, pp. 103–109, 2013.
- [24] M. M. Tom Scherer, “Using Electrical Conductivity and Total Dissolved Solids Meters to Field Test Water Quality,” North Dakota State University Extension.<https://www.ndsu.edu/agriculture/extension/publications/using-electrical-conductivity-and-total-dissolved-solids-meters-field-test>, [Online] Accessed: 18-June-2023.
- [25] “What is the relationship between TDS and EC?” HANNA instruments.<https://knowledge.hannainst.com/en/knowledge/ec-tds-what-is-the-relationship-between-tds-and-ec>, [Online] Accessed: 1-July-2023.

- [26] “Mini Conductivity K 1.0 Kit,” Atlas Scientific.<https://atlas-scientific.com/kits/mini-conductivity-k-1-0-kit/>, [Online] Accessed: 18-June-2023.
- [27] “How Do Conductivity Meters Work?” Atlas Scientific.<https://atlas-scientific.com/blog/how-do-conductivity-meters-work/>, [Online] Accessed: 30-June-2023.
- [28] J. L. M. R. K. R. P. W. B. Alberts, A. Johnson, Molecular Biology of the Cell. USA: Garland Science, March 2002.
- [29] J. Zhou, P. Li, J. Wang, and W. Fu, “Growth, photosynthesis, and nutrient uptake at different light intensities and temperatures in lettuce,” HortScience, vol. 54, no. 11, pp. 1925–1933, 2019.
- [30] S. Barbi, F. Barbieri, A. Bertacchini, L. Barbieri, and M. Montorsi, “Effects of different led light recipes and npk fertilizers on basil cultivation for automated and integrated horticulture methods,” Applied Sciences, vol. 11, no. 6, p. 2497, 2021.
- [31] W. Tang, H. Guo, C. C. Baskin, W. Xiong, C. Yang, Z. Li, H. Song, T. Wang, J. Yin, X. Wu et al., “Effect of light intensity on morphology, photosynthesis and carbon metabolism of alfalfa (*medicago sativa*) seedlings,” Plants, vol. 11, no. 13, p. 1688, 2022.
- [32] J. Zhou, J. Wang, T. Hang, P. Li et al., “Photosynthetic characteristics and growth performance of lettuce (*lactuca sativa l.*) under different light/dark cycles in mini plant factories,” Photosynthetica, vol. 58, no. 3, pp. 740–747, 2020.
- [33] M. T. Naznin, M. Lefsrud, M. O. K. Azad, and C. H. Park, “Effect of different combinations of red and blue led light on growth characteristics and pigment content of in vitro tomato plantlets,” Agriculture, vol. 9, no. 9, p. 196, 2019.
- [34] “Auoyo 20W 40W Pl-ant Lights Growing Lamps Red Blue LED Full Spectrum Indoor Pl-anting 169 LED Grow Lamp For Succulent Vegetable Flower Glow EU Plug,” Daraz.<https://www.daraz.com.bd/products/auoyo-20w-40w-pl-ant-lights-growing-lamps-red-blue-led-full-spectrum-indoor-pl-anting-169.html>, [Online] Accessed: 20-June-2023.

- [35] “BH1750 Ambient Light Sensor,” <https://learn.adafruit.com/adafruit-bh1750-ambient-light-sensor/overview>, [Online] Accessed: 10-July-2023.
- [36] “What Is pH? The pH Formula Equation,” Chemistrytalk.<https://chemistrytalk.org/what-is-ph/>, [Online] Accessed: 20-June-2023.
- [37] D. Neina, “The role of soil ph in plant nutrition and soil remediation,” Applied and environmental soil science, vol. 2019, pp. 1–9, 2019.
- [38] “Soil pH,” Agriculture Victoria.https://vro.agriculture.vic.gov.au/dpi/vro/vrosite.nsf/pages/soilhealth_ph, [Online] Accessed: 20-June-2023.
- [39] “Atlas Scientific pH Kit,” Atlas Scientific.<https://atlas-scientific.com/kits/ph-kit/>, [Online] Accessed: 28-June-2023.
- [40] “Environmental factors affecting plant growth,” Oregon State University Extension Service.<https://extension.oregonstate.edu/gardening/techniques/environmental-factors-affecting-plant-growth>, [Online] Accessed: 26-June-2023.
- [41] H. C. Thompson, R. W. Langhans, A.-J. Both, and L. D. Albright, “Shoot and root temperature effects on lettuce growth in a floating hydroponic system,” Journal of the American Society for Horticultural Science, vol. 123, no. 3, pp. 361–364, 1998.
- [42] M. Hasanuzzaman, K. Nahar, M. M. Alam, R. Roychowdhury, and M. Fujita, “Physiological, biochemical, and molecular mechanisms of heat stress tolerance in plants,” International journal of molecular sciences, vol. 14, no. 5, pp. 9643–9684, 2013.
- [43] C. E. Moore, K. Meacham-Hensold, P. Lemonnier, R. A. Slattery, C. Benjamin, C. J. Bernacchi, T. Lawson, and A. P. Cavanagh, “The effect of increasing temperature on crop photosynthesis: from enzymes to ecosystems,” Journal of Experimental Botany, vol. 72, no. 8, pp. 2822–2844, 2021.
- [44] “Growing-on at Cooler than Optimum Temperatures,” UMass Extension Greenhouse Crops and Floriculture Program.<https://ag.umass.edu/greenhouse-floriculture/fact-sheets/>

- growing-on-at-cooler-than-optimum-temperatures, [Online] Accessed: 26-June-2023.
- [45] “DHT22 temperature-humidity sensor + extras,” Adafruit.<https://www.adafruit.com/product/385>, [Online] Accessed: 30-June-2023.
- [46] “DHT11 DHT22 Sensors Temperature and Humidity Tutorial using Arduino,” How To Mechatronics.<https://howtomechatronics.com/tutorials/arduino/dht11-dht22-sensors-temperature-and-humidity-tutorial-using-arduino/>, [Online] Accessed: 28-June-2023.
- [47] K. Pregitzer and J. King, “Effects of soil temperature on nutrient uptake,” Nutrient acquisition by plants: an ecological perspective, pp. 277–310, 2005.
- [48] “Plant responses to cold,” Plants in Action.<https://www.rseco.org/content/145-plant-responses-cold.html>, [Online] Accessed: 26-June-2023.
- [49] J. L. Hatfield and J. H. Prueger, “Temperature extremes: Effect on plant growth and development,” Weather and climate extremes, vol. 10, pp. 4–10, 2015.
- [50] “Guide for DS18B20 Temperature Sensor with Arduino,” Random Nerd Tutorials.<https://randomnerdtutorials.com/guide-for-ds18b20-temperature-sensor-with-arduino/>, [Online] Accessed: 28-June-2023.
- [51] T. L. Stockstad, “Temperature-to-digital converter,” Patent US6 847 319B1, 2003.
- [52] “DS18B20 Programmable Resolution 1-Wire Digital Thermometer,” Analog Devices.<https://www.analog.com/en/products/ds18b20.html#product-overview>, [Online] Accessed: 30-June-2023.
- [53] M. A. FORD and G. N. Thorne, “Effects of atmospheric humidity on plant growth,” Annals of Botany, vol. 38, no. 2, pp. 441–452, 1974.
- [54] D. Taub, “Effects of rising atmospheric concentrations of carbon dioxide on plants,” Nature Education Knowledge, vol. 1, no. 8, 2010.

- [55] M. Thompson, D. Gamage, N. Hirotsu, A. Martin, and S. Seneweera, “Effects of elevated carbon dioxide on photosynthesis and carbon partitioning: a perspective on root sugar sensing and hormonal crosstalk,” *Frontiers in Physiology*, p. 578, 2017.
- [56] Z. Xu, Y. Jiang, B. Jia, and G. Zhou, “Elevated-co₂ response of stomata and its dependence on environmental factors,” *Frontiers in plant science*, vol. 7, p. 657, 2016.
- [57] Winsen Sensor, “Infrared CO₂ Sensor Module (Model: MH-Z19C) User’s Manual,” https://www.winsen-sensor.com/d/files/infrared-gas-sensor/mh-z19c-pins-type-co2-manual-ver1_0.pdf, 2020, zhengzhou Winsen Electronics Technology Co., Ltd.
- [58] L. E. Peterson, “K-nearest neighbor,” *Scholarpedia*, vol. 4, no. 2, p. 1883, 2009.
- [59] M. Mehra, S. Saxena, S. Sankaranarayanan, R. J. Tom, and M. Veeramanikandan, “Iot based hydroponics system using deep neural networks,” *Computers and electronics in agriculture*, vol. 155, pp. 473–486, 2018.
- [60] T. Chen and C. Guestrin, “Xgboost: A scalable tree boosting system,” in *Proceedings of the 22nd acm sigkdd international conference on knowledge discovery and data mining*, 2016, pp. 785–794.
- [61] T. G. Dietterich, “Ensemble methods in machine learning,” in *International workshop on multiple classifier systems*. Springer, 2000, pp. 1–15.
- [62] R. Shwartz-Ziv and A. Armon, “Tabular data: Deep learning is not all you need,” *Information Fusion*, vol. 81, pp. 84–90, 2022.
- [63] T.-H. Lee, A. Ullah, and R. Wang, “Bootstrap aggregating and random forest,” *Macroeconomic forecasting in the era of big data: Theory and practice*, pp. 389–429, 2020.
- [64] X. Yang, Y. Wang, R. Byrne, G. Schneider, and S. Yang, “Concepts of artificial intelligence for computer-assisted drug discovery,” *Chemical reviews*, vol. 119, no. 18, pp. 10520–10594, 2019.

- [65] Y. Freund and R. E. Schapire, “A decision-theoretic generalization of on-line learning and an application to boosting,” *Journal of computer and system sciences*, vol. 55, no. 1, pp. 119–139, 1997.
- [66] R. Guo, Z. Zhao, T. Wang, G. Liu, J. Zhao, and D. Gao, “Degradation state recognition of piston pump based on iceemdan and xgboost,” *Applied Sciences*, vol. 10, no. 18, p. 6593, 2020.
- [67] E. J. Ryder and T. W. Whitaker, “*Lactuca sativa*: En. lettuce; fr. laitue; ge. lattich, salat; sp. lechuga,” in *CRC Handbook of Flowering*. CRC Press, 2019, pp. 241–245.
- [68] Z. F. Ahmed, A. K. Alnuaimi, A. Askri, and N. Tzortzakis, “Evaluation of lettuce (*lactuca sativa* l.) production under hydroponic system: Nutrient solution derived from fish waste vs. inorganic nutrient solution,” *Horticulturae*, vol. 7, no. 9, p. 292, 2021.
- [69] C. S. Dr. Melissa Brechner, Dr. A.J. Both, *Hydroponic Lettuce Handbook*. New York, USA: Cornell University Controlled Environment Agriculture Program, 2013.
- [70] M. D’Anna, S. Groot, M. Joyce, and S. Palmer, “Automated hydroponic greenhouse,” University of Massachusetts, Massachusetts, 2016.
- [71] R. Maiza and D. Kurnia, “The influence of light wavelengths toward the growth of *brassica rapa* l.” in *Journal of Physics: Conference Series*, vol. 1245, no. 1. IOP Publishing, 2019, p. 012089.
- [72] K. Kularbphetpong, U. Ampant, and N. Kongrodj, “An automated hydroponics system based on mobile application,” *International Journal of Information and Education Technology*, vol. 9, no. 8, pp. 548–552, 2019.
- [73] D. Adidrana and N. Surantha, “Hydroponic nutrient control system based on internet of things and k-nearest neighbors,” in *2019 International Conference on Computer, Control, Informatics and its Applications (IC3INA)*. IEEE, 2019, pp. 166–171.
- [74] M. Griffiths, “The design and implementation of a hydroponics control system,” 2014.

- [75] D. S. Domingues, H. W. Takahashi, C. A. Camara, and S. L. Nixdorf, “Automated system developed to control ph and concentration of nutrient solution evaluated in hydroponic lettuce production,” Computers and electronics in agriculture, vol. 84, pp. 53–61, 2012.
- [76] R. T. Michael Sweat and R. Hochmuth, “BUILDING A FLOATING HYDROPONIC GARDEN,” University of Florida Institute of Food and Agricultural Sciences Extension. <https://edis.ifas.ufl.edu/publication/HS184>, [Online] Accessed: 10-April-2023.
- [77] K. Cheng and D.-M. Zhu, “On calibration of ph meters,” Sensors, vol. 5, no. 4, pp. 209–219, 2005.
- [78] “Gravity: Analog pH Sensor/Meter Kit V2 (Arduino Raspberry Pi micro:bit Compatible),” DFRobot.<https://www.dfrobot.com/product-1782.html>, [Online] Accessed: 20-June-2023.
- [79] “SEN0244 Gravity Analog TDS Sensor Meter For Arduino,” DFROBOT.https://wiki.dfrobot.com/Gravity_Analog_TDS_Sensor_Meter_For_Arduino_SKU_SEN0244, [Online] Accessed: 30-June-2023.
- [80] “HC-SR04 Ultrasonic Sonar Distance Sensor + 2 x 10K resistors,” Adafruit.<https://www.adafruit.com/product/3942>, [Online] Accessed: 30-June-2023.
- [81] Lenovo, “Lenovo Select FHD Webcam ,” Lenovo, , [Online] Accessed: 1-January-2024. [Online]. Available: https://www.lenovo.com/us/en/p/accessories-and-software/webcams-and-video/webcams-and-video_webcams/gxc1d05522?orgRef=https%253A%252F%252Fwww.google.com%252F
- [82] “TEC1-12706 Thermoelectric Peltier Cooling Device,” Proto Supplies.<https://protosupplies.com/product/tec1-12706-thermoelectric-peltier-cooling-device/>, [Online] Accessed: 30-June-2023.
- [83] Hebei I.T. (Shanghai) Co., Ltd, “TEC1-12715 Datasheet,” Hebei I.T. (Shanghai) Co., Ltd, , [Online] Accessed: 16-September-2023. [Online]. Available: <https://peltiermodules.com/peltier.datasheet/TEC1-12715.pdf>

- [84] “Submersible 3V DC Water Pump - 1 Meter Vertical Type,” Adafruit.<https://www.adafruit.com/product/4547>, [Online] Accessed: 1-July-2023.
- [85] H. A. Ahmed, T. Yu-Xin, and Y. Qi-Chang, “Optimal control of environmental conditions affecting lettuce plant growth in a controlled environment with artificial lighting: A review,” South African Journal of Botany, vol. 130, pp. 75–89, 2020.
- [86] ImageJ, “Fiji,” ImageJ, , [Online] Accessed: 1-January-2024. [Online]. Available: <https://imagej.net/software/fiji/>

Appendix A: List of Acronyms

GM Growth Module

NSCM Nurient Solution Container Module

IoT Internet of Things

KNN K-Nearest Neighbour

GUI Graphical User Interface

CO₂ Carbon Dioxide

LED Light and Emitting Diode

pH Potential Hydrogen

EC Electrical and Conductivity

TDS Total Dissolved Solids

NFT Nutrient Film Technique